In: Earthquakes
Editor: Kostas Konstantinou
ISBN: 978-1-62081-883-1

Chapter 1

COASTAL TECTONIC STRAIN AND PALEOSEISMICITY IN THE SOUTH CENTRAL CASCADIA MARGIN, OREGON, US

Curt D. Peterson, Kenneth M. Cruikshank and Mark E. Darienzo*

Department of Geology, Portland State University, Portland, OR, US

ABSTRACT

Four different geologic records are compared for evidence of convergent tectonic strain in the South Central Cascadia Margin (500 km in length), Oregon, USA. The strain records represent widely different time scales, including late Neogene, late Pleistocene, late Holocene, and modern time scales. Modern strain records are taken from global position system (GPS) data complied from three representative localities, positioned north, central and south in the study area at 1-50 km distance landward of the coast. These modern GPS data show convergent shortening rates of 5-9 mm yr^{-1} over 40 km west–east baselines. The southernmost GPS stations also demonstrate an along coast shortening trend that is consistent with oblique convergence in the southernmost part of the study area. Late Neogene records of convergent strain are represented by west and east dip angles of middle Miocene to Eocene sedimentary rocks. Background dip angles (10-20°) increase to 30-60° at distances of less than 90 km from the deformation front in the central part of the study area. The elevations of late Pleistocene high sea level stand deposits (80–120 ka in age) are measured at 76 sites along the study area coastline. Background variability of the sea level high stand deposits (±4 m 1–σ) increases to ±11 m 1–σ at distances of less than 75 km from the deformation front. The late Neogene and late Pleistocene deformation is assumed to reflect inelastic strain associated with local upper plate folds and faults near the interplate coupled zone. Late-Holocene records of episodic tidal marsh subsidence (0.5–1.5 m) in 33 representative core sites from 7 estuaries establish the regional trough of elastic coseismic subsidence. The distance between the trough of maximum coseismic subsidence (1.5 m subsidence) and the deformation front narrows from 150 km in the north to 100 km in the south of the study

* Department of Geology, Portland State University, PO Box 751, Portland, OR 97207-0751.

area. These across margin distances demonstrate a relatively wide zone of episodic interplate coupling throughout the length of the South Central Cascadia Margin. All four coastal records, including modern GPS strain, late Neogene deformation, late Pleistocene deformation, and late Holocene episodic subsidence reflect convergent strain associated with subduction of the Juan De Fuca oceanic plate under the North American continental plate.

INTRODUCTION

The South Central Cascadia Margin, defined here by the southern onehalf of the subducting Juan De Fuca plate (Figure 1) demonstrates convergent tectonic strain over different time and length scales. Late Holocene records of coastal subsidence [Darienzo and Peterson 1990**;** Darienzo et al., 1994] and associated nearfield paleotsunami inundations [Atwater et al., 1995; Peterson and Darienzo, 1997; Peterson et al., 2008] indicate prehistoric occurrences of megathrust ruptures in the South Central Cascadia Margin.

Unlike the well developed sequences of coseismic coastal subsidence in Willapa Bay and Grays Harbor in the North Central Cascadia Margin [Atwater et al., 2004] (Figure 1) the records of episodic coastal subsidence diminish to below detection in some small estuaries of the South Central Cascadia Margin [Briggs, 1994; Peterson et al., 2000].

These poorly developed records of coastal subsidence have led some investigators [Nelson, 1987; 1992; Shennan et al., 1998] to argue against through going megathrust ruptures in the South Central Cascadia Margin.

A likely contributing factor to the along coast variability of episodic coastal subsidence in the South Central Cascadia Margin is the orientation of the coastline, relative to the buried subduction zone trench, or deformation front (Figure 1). The across margin distances between the shoreline and the deformation front decrease from about 120 to 75 km with distance south along the 500 km coastline in the study area. Along coast changes in plate convergence angles and oceanic plate thermal gradients [Hyndman and Wang, 1995] add further difficulties to the assessment of seismic hazards in the South Central Cascadia Margin.

In this chapter four different geologic records of convergent plate tectonic strain are examined in the South Central Cascadia Margin (Figure 1). These records include 1) modern strain rates from continuously monitored GPS stations, 2) late Neogene deformation of coastal sedimentary rocks, 3) vertical deformation of late Pleistocene marine terraces, and 4) late Holocene records of episodic coastal subsidence. The coastal deformation is related to 1) inelastic strain in the upper plate deformation belt and 2) elastic strain recorded in the trough of cosesismic subsidence, which slightly overlaps the seaward extents of the upper plate deformation belts. These relationships can be used to define the interplate coupled zone, which episodically ruptures to produce megathrust earthquakes and associated nearfield tsunami in the South Central Cascadia margin.

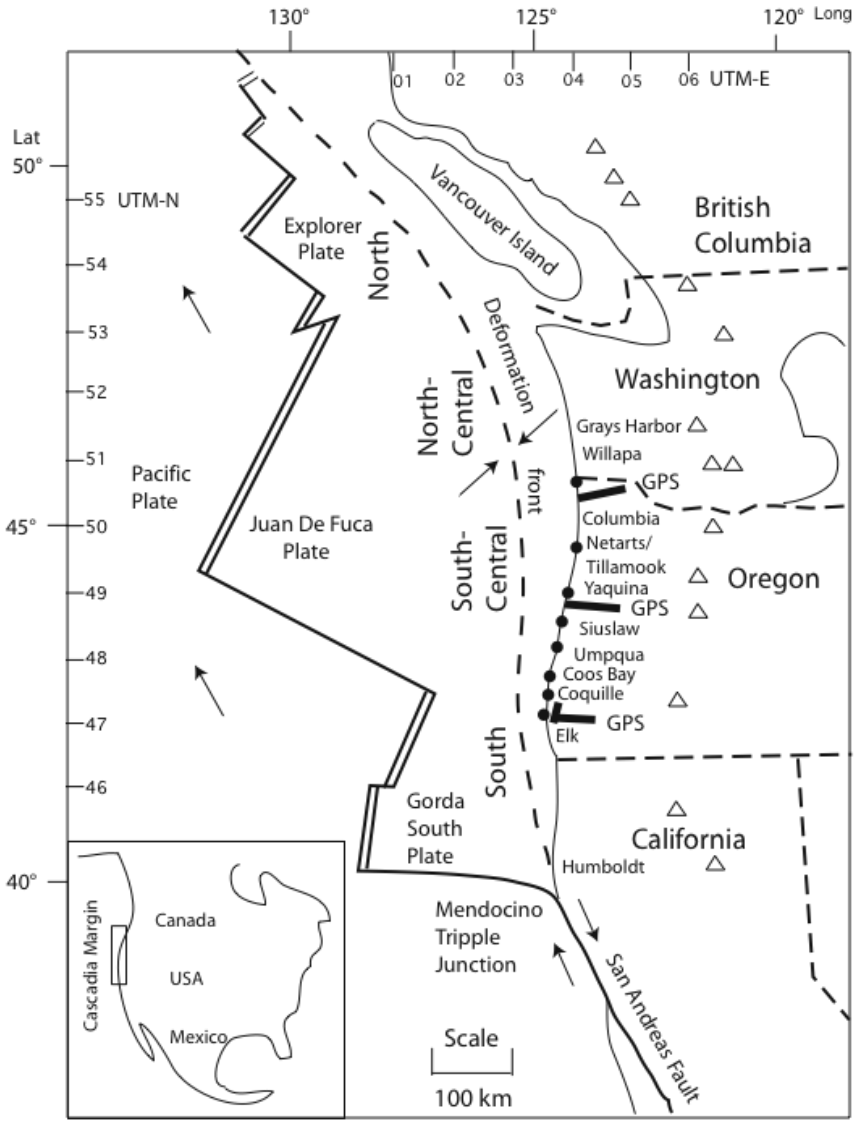

Figure 1. Cascadia margin coastline (solid line), buried trench or deformation front (dashed line), and continental volcanic arc (open triangles). Arrows represent directions of plate convergence with a reported convergence rate of about four centimeters per year in the central Cascadia margin. Convergence becomes increasingly oblique with proximity to the San Andreas transform fault located south of the Mendocino triple junction. For this paper the Central Cascadia margin is defined by the extent of the Juan De Fuca Plate segment. The South Central Cascadia margin is contained in the State of Oregon, located south of the Columbia River. Tidal basins recording late Holocene records of episodic coastal subsidence (solid circles) in the South Central Cascadia Margin are named. Modern GPS strain traverses (bold lines) are shown for the north, central, and southern parts of the study area. Map coordinates are in degrees latitude and longitude and in 100 km intervals in UTM zone 10.

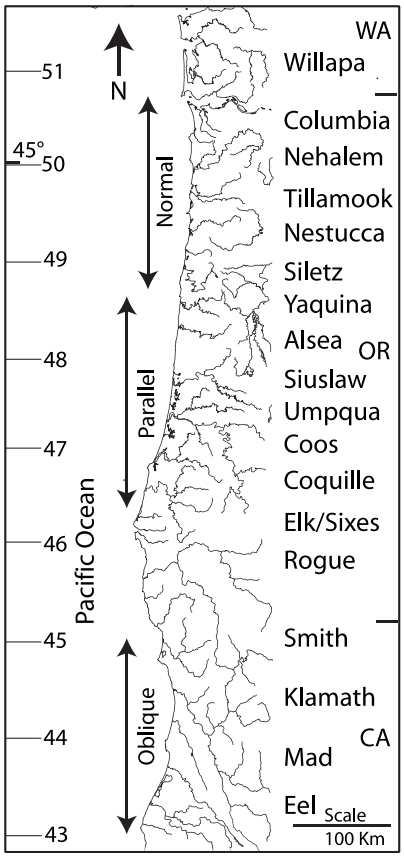

Figure 2. Coastal river valley orientations in the South Central and South Cascadia margin. Coastal drainages transition from oblique to parallel to normal or perpendicular with increasing distance north along the 800 km long coastline. See Figure 5 in the Results section for larger scale maps of the coast parallel drainages in the south central part of the study area. Map coordinates are in degrees latitude and 100 km intervals UTM zone 10.

STUDY AREA AND PREVIOUS WORK

Observations of coastal stream alignments and uplifted Pleistocene marine terraces in the South Central Cascadia Margin led to early searches for compressive strain accumulation that could be recorded in uplifted estuarine deposits [Peterson and Scheidegger, 1984]. Events of episodic coastal subsidence were subsequently found in late Holocene tidal wetland deposits, which are developed in submerged river valleys of the South Central Cascadia Margin [Darienzo, 1987**;** Darienzo and Peterson, 1990**;** Darienzo et al., 1994]. Strikes and dips of coastal sedimentary rocks are exposed in river and road cuts that follow the coastal river valleys landward from the estuaries [Baldwin, 1956, 1961, 1974; Snavely et al., 1972a,b; Newton, 1980]. For these reasons the coastal strain records that are discussed in this chapter are loosely organized around estuaries and their associated tributary drainages (Figure 2).

In the South Cascadia margin, which is located landward of the Gorda Plate segment (Figure 1) the coastal river valleys trend northwest. The coastal rivers intersect the coastline

at oblique angles (Figure 2). The river valleys are approximately aligned with northwest–southeast trending thrust faults. The thrust faults are thought to reflect oblique subduction, which is expected to occur north of the Mendocino triple junction. Late Holocene records of episodic coastal subsidence or uplift in Humboldt Bay in the South Cascadia Margin (Figure 1) are localized on upper plate structures, which are likely to be associated with the active thrust faults [Clarke and Carver, 1992**;** Li, 1992].

The southern part of the South Central Cascadia Margin contains coastal streams (Figure 2) that are characterized by trellis patterns. These streams are aligned with north–south trending folds. The coast parallel trends or meanders of the stream valleys only extend 5-20 km landward of the shoreline, before realigning to east–west dendritic patterns in the Coast Range. Late Holocene marsh deposits in some of the fold axis valleys, such as South Slough in Coos Bay, demonstrate episodic subsidence [Darienzo and Peterson, 1987; Nelson et al., 1996]. However, other salt marsh deposits in the lower reaches of Coos Bay and in nearby estuaries of the Umpqua and Siuslaw Rivers contain little or no record of episodic wetland submergence [Briggs, 1994].

Coastal streams in the northern part of the South Central Cascadia Margin form dendritic drainages that are generally aligned normal or perpendicular to the coastline (Figure 2). Salt marsh deposits in the submerged lower reaches of these river valleys show evidence of episodic subsidence, but the cyclic emergence and submergence values are modest (< 1.0 m relative to paleosea level datums) [Barnett, 1997; Peterson et al., 2000]. Some investigators have argued that such weak subsidence records are indistinguishable from aseismic submergence processes and that they do not necessarily demonstrate through-going megathrust ruptures in the South Central Cascadia Margin [Shennan et al., 1998].

West and McCrumb [1988] used low-uplift rates (0.1–0.2 mm yr^{-1}) of coastal marine terraces (80 ka) in the Central Cascadia Margin to argue against megathrust coupling. However, offshore seismic reflection mapping, as compiled by Peterson and Gray [1986] reveals a prominent fold and fault belt that approximately parallels the deformation front (Figure 3). The deformation belt extends from the deformation front or buried trench to the landward reach of the fold and fault belt, as mapped by offshore seismic profiling. The deformation belt extends 110 km east of the deformation front offshore of the Columbia River, but appears to intersect the coastline south of Coos Bay, at ~ 80 km from the deformation front in the southern part of the study area [Peterson and Gray, 1986].

Oblique, northwest trending strike slip faults cut across the offshore deformation belt (Figure 3). Those oblique faults are left lateral [Goldfinger, et al., 1992a]. Northwest trending faults are also mapped in onshore Miocene rocks in the northern part of the study area [Niem and Niem, 1985; Peterson and Gray, 1986]. However, the onshore faults are right lateral strike-slip faults [Wells, 1990] so they are not connected to deformation in the offshore fold and fault belt. The discontinuity between the offshore and onshore strike slip faults occurs within a distance of 60-90 km from the deformation front in the central study area.

The most prominent features in the offshore deformation belt are north–south trending fold axes (Figure 3). Extensive seismic profiling, side-scan sonar, and submersible diving in the early 1990s confirmed an abundance of Quaternary folds and faults in the offshore deformation belt [Goldfinger, et al., 1992b]. Late Pleistocene, shore-parallel folds are mapped to within 10-20 km of the coastline in northernmost part of the study area, but they appear to obliquely intersect the coast in the vicinity of Coos Bay in the southern part of the study area.

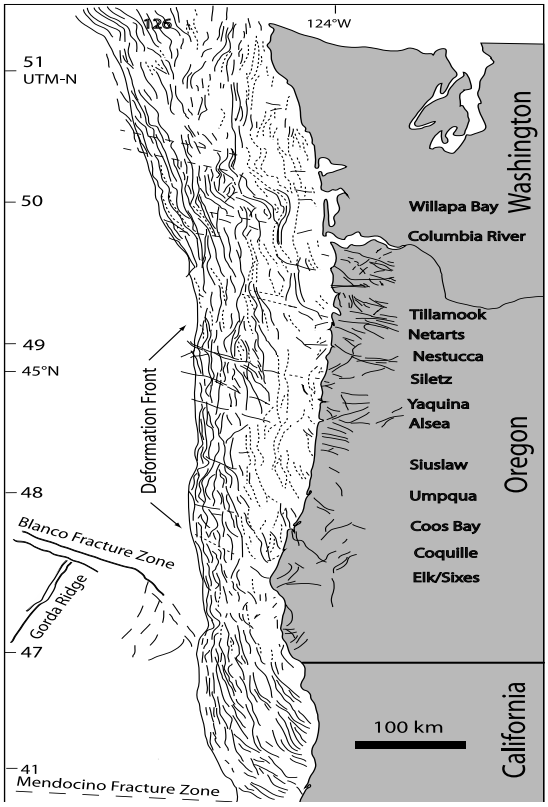

Figure 3. Map of folds (lines) and faults (bold lines) in the offshore fold and thrust belt (between shoreline and deformation front) and in Tertiary bedrock formations (located landward of the shoreline) in the Central and South Cascadia Margin. Onshore Tertiary faults are redrafted from Peterson and Gray [1986]. Pleistocene folds and faults (lines) and inferred folds and faults (dashed lines) in the offshore deformation belt are from Goldfinger et al., [1992a; 1996; 1992b] as compiled by McNeil, et al. [1998]. Map coordinates are in degrees latitude and 100 km intervals UTM zone 10.

The most current investigations of late Holocene paleoseismic indicators in the South Central Cascadia Margin have focused on continental slope turbidites [Goldfinger et al., 2008] and on overland paleotsunami inundation [Peterson et al., 2010]. These indirect records of subduction zone seismicity indicate the occurrences of megathrust ruptures with mean recurrence intervals of ~ 350–500 years. Some of the possible ruptures are correlated along the full length of the South Central Cascadia Margin, suggesting earthquake magnitudes of Mw 8.5-9.0. How can these paleoseismic indicators be reconciled with interpretations of little or no interplate coupling in parts of the South Central Cascadia Margin?

RESULTS

In this chapter the geologic records of tectonic strain are compared to reconcile the different interpretations of megathrust coupling and coseismic rupture in the South Central Cascadia Margin. The first report on modern GPS strain records in the South Central Cascadia Margin are followed by long term records of inelastic coastal deformation

associated with intermittent megathrust coupling. The chapter transitions to elastic records of strain with overviews of late Holocene records of cyclic interseismic uplift and coseismic subsidence. These records of the elastic strain cycles define the trough of coseismic subsidence, located above and landward of the interplate coupled zone. The chapter concludes with a return to the modern strain evidence as provided by GPS stations located 1-50 km landward of the coast.

Modern GPS Strain Records

Three GPS localities are selected for modern GPS strain records in the vicinities of the Columbia River (Seaside), Yaquina–Alsea Rivers (Newport), and Coquille (Bandon) in the South Central Cascadia Margin (Figures 1 and 2). The three localities represent the north, central, and southern parts of the study area. Several GPS stations are used for each locality (triangular networks) to verify results between adjacent baselines. Additional GPS stations (Cape Blanco and Coos Bay) that are located are either side of Bandon are also selected to test for north–south shortening in the southern part of the study area. The GPS station positions are analyzed for changes in station to station distance through time (3 years) depending on the duration of consistent continuous coverage (PNGA, 2011; NOAA, 2011). The GPS traverses or baselines are selected to include stations that are located at the coast and at about 40–50 km distance inland from the coast (Table 1).

The data from the continuously operating GPS stations (CORS, 2011; PANGA, 2011) were accessed and baselines between pairs of stations were processed in the period 2006 to 2011 using utilities in the GPStk software package [Tolman et al., 2004]. The Vecsol component of the GPStk package solves for the distance between stations; using this result rather than coordinates allows determination of strains without ambiguities introduced by coordinate transformations. Statistical analysis on the change in baseline lengths was performed using R statistical software [R Development Core Team, 2011] and the MASS analysis library [Venables and Ripley, 2002]. An Analysis of Variance (ANOVA) test on the regression shows that the slope of the change of baseline with time is significant ($\alpha = 0.05$, null hypothesis is that the slope of the regression is zero, alternate hypothesis is that slope is different from zero), indicating there is a significant trend. All the baselines presented here showed a significant trend in the change in distance between the two stations (Table 1, Figure 4).

These data (Table 1) show that there is significant west–east shortening throughout the length of the South Central Cascadia Margin. The change in west–east baseline length in the Seaside locality, near the Columbia River, is 7–8 mm yr^{-1} for the 50–55 km long baselines (Figure 4). Apparent cycling in the strain rates might be due to seasonal atmospheric variability. The change in west–east baseline lengths in the Newport locality in the central part of the study area is about 5 mm yr^{-1} for 38–44 km long baselines. The change in west–east baseline length in the Bandon locality in the southern part of the study area is about 9 mm for the 39 km long baseline.

Table 1. Summary of preliminary strain observations for selected parts of the Oregon coast

'From' Station	'To' Station		Baseline Length (m)	Change in length (mm a^{-1})	Strain Rate (a^{-1})
Northern Oregon					
Seaside (P407)	Whakiakum, WA (P408)		50853	-8.132	-1.6×10^{-7}
Seaside (P407)	Vernonia, OR (P409)		54878	-7.116	-1.3×10^{-7}
Central Oregon					
Ona Beach, OR (ONAB)	Alsea, OR (P374)		41238	-4.969	-1.2×10^{-7}
Newport Airport, OR (P367)	Alsea, OR (P374)		43749	-4.883	-1.1×10^{-7}
Alsea, OR (P374)	Halsey, OR (HLSY)		38349	-3.201	-8.3×10^{-8}
Southern Oregon					
Cape Blanco, OR (CABL)	Bandon Airport, OR (P364)		30913	-7.542	-2.4×10^{-7}
Cape Blanco, OR (CABL)	Coos Bay, OR (P365)		67070	-10.937	-1.6×10^{-7}
Bandon Airport, OR (P364)	Powers, OR (P363)		38653	-8.832	-2.3×10^{-7}
Bandon Airport (P364)	Coos Bay, OR (P365)		36190	-6.794	-1.9×10^{-7}
Site	Station ID	Latitude	Longitude	UTM East	UTM North
Whakiakum, WA	p408	46.2004	-123.3764	470961	5116378
Seaside, OR	p407	45.9546	-123.9306	427886	5089427
Vernonia, OR	p409	45.8511	-123.2393	481422	5077536
Newport Airport, OR	p367	44.5852	-123.9384	425505	4937306
Ona Beach, OR	onab	44.5154	-124.0732	414702	4929674
Alsea, OR	p374	44.3819	-123.5904	452967	4914457
Halsey, OR	hlsy	44.3775	-123.1089	491325	4913803
Coos Bay, OR	p365	43.3953	-124.2533	398505	4805479
Bandon Airport, OR	p364	43.0902	-124.4091	385314	4771789
Powers, OR	p363	42.8599	-124.0538	413907	4745798
Cape Blanco, OR	cabl	42.8361	-124.5633	372238	4743799

Trends for some baselines are shown in Figure 4. The baselines all became significantly shorter over the 2007–2011 period, with strain rates ranging from -8.3×10^{-8} to -2.3×10^{-7}.

a^{-1} which yields changes in lengths in the order of 5 mm over a 40 km baseline.

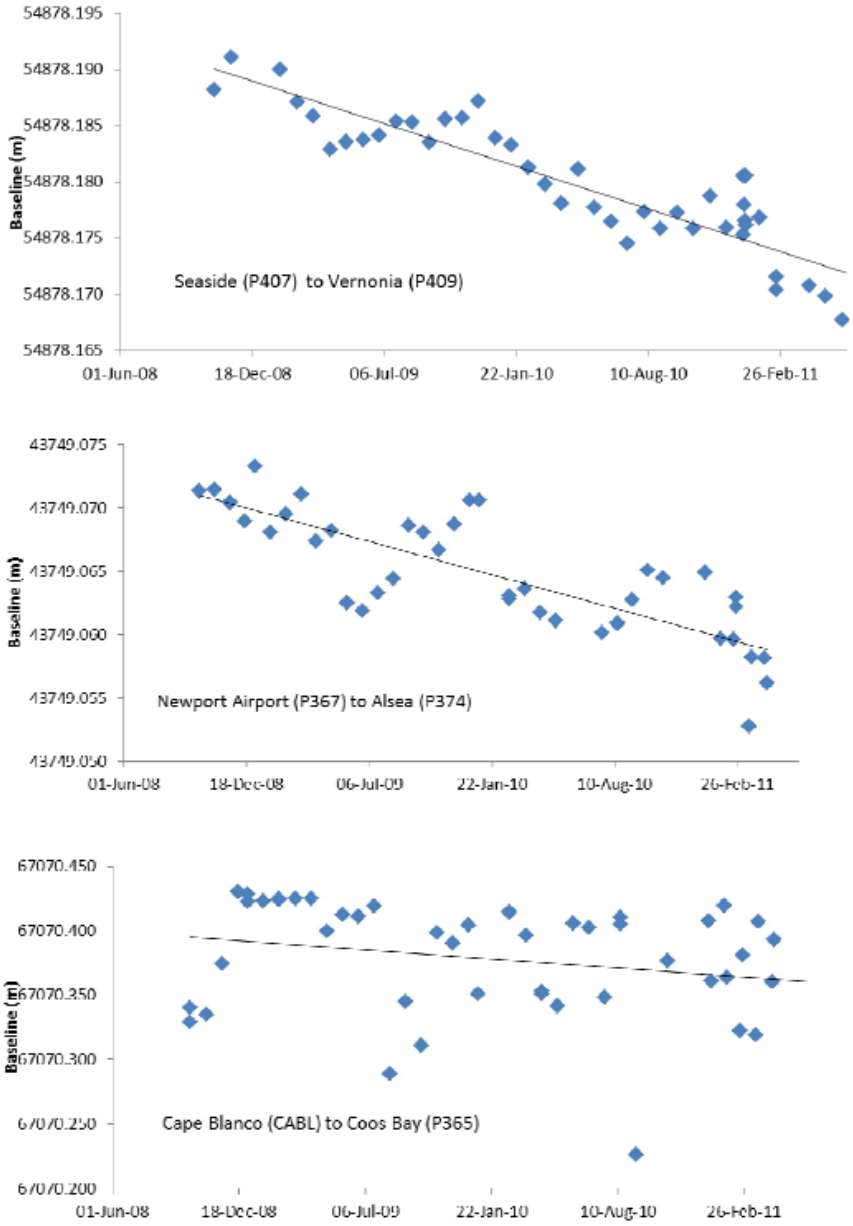

Figure 4. Representative trends in baseline lengths for the Seaside-Columbia River GPS locality (top plot), Newport-Yaquina/Alsea locality (middle plot), and Cape Blanco-Coquille-Coos Bay locality (bottom plot). See Figure 1 for approximate locations and Table 1 for calculated strain results). The west–east baselines all show significant shortening (a=0.05).

To test for south–north strain in the south coast, possibly associated with oblique convergence or south–north compression from the San Andreas transform fault (Figure 1) two south–north baselines are analyzed. Both end to end baselines (31-36 km in length), record about 7 mm yr^{-1} of shortening, suggesting that the accumulated south-north strain in the south coast is occurring regionally, rather than in a specific upper plate structure.

Late-Neogene Strain Records

Late-Neogene regional uplift of an Eocene embayment terminated marine sediment deposition and created the present Coast Range in the South Central Cascadia margin. Miocene strata in the northern Coast Range drainages give way to older Eocene strata in the southern drainages. River valley erosion has dissected the Miocene-Eocene marine strata, which have been deformed by late Neogene uplift, rotation and/or compression [Niem and Niem, 1985; Wells, 1990; Black, 1993]. The record of west–east crustal shortening from convergent strain is of greatest concern to this study. Narrow traverses in selected drainages are compiled for dip angles within 45° of west or east in Miocene–Eocene strata located between 1 and 30 km of the coastline. Such dip angles could reflect north–south trending folds, ramps, and/or thrust faults. The compiled bedrock strikes and dips were originally mapped for oil and gas surveys [Baldwin, 1956; Baldwin, 1961; Snavely et al., 1972a,b; Baldwin et al., 1973; Baldwin, 1974; Schlicker and Deacon, 1974, Newton, 1980].

A preliminary examination of the Eocene strata in the south central drainages including the Siuslaw, Tahkenitch, Umpqua, Ten Mile, and Coos Drainages (Figure 5) showed modest west–east dip angles (mean 13° ± 10° 1–σ N=246) when averaged over the ~ 25 km long traverses. The lowest dip angles (3–6° W) that are found at the eastern ends of the south–central drainage traverses are thought to reflect broad late Neogene uplift of the Coast Range. Bedrock strata in the northern drainages are dominated by Miocene sedimentary rocks [Snavely et al., 1972a,b; Niem and Niem, 1985]. Averaged west–east dip angles (mean 13° ± 5° 1–σ N=52) from the northern Siletz traverse (Figure 3) are similar to those in the south central drainages. However, there are no consistent changes in west–east dip angles with distance from the coast in the Siletz traverse [Snavely et al., 1972a,b] or in the northernmost Tillamook drainages of the study area [Niem and Niem, 1985]. Bedrock strata in the southernmost drainages, south of Coos Bay (Figure 3), contain both Tertiary and Mesozoic rocks [Baldwin et al., 1973; Baldwin, 1974]. East and west dip angles from the late Eocene sedimentary rocks within 25 km of the coast in the Coquille drainage (Figure 3) are substantially greater (mean 51° ± 15° 1–σ N=50) than those in the central drainages. There are no consistent changes in west–east dip angles within 25 km distance from the coast in the Coquille drainage [Baldwin et al., 1973]. Only the south–central drainages of the study area both 1) contain low dip angles (< 10° dip) within 25 km of the coast and 2) demonstrate increasing dip angles with increasing proximity to the coastline (Figure 5).

The five south central traverses selected for documentation of late Neogene convergent strain records (Figure 5) demonstrate patterns of increasing west–east dips from east to west.

Anomalous dip angles are clustered within and between the five localities, but the overall trend is that of increasing fold and/or fault deformation towards the coastline. For example, west–east dip angles increase from about 5° to 30° over a westward distance of 20 km in the northern Siuslaw locality (Figure 5a). Dip angles increase from about 5° to 20° over 15-20 km distances in the Tahkenitch, Umpqua, and Ten Mile localities (Figures 5b, 5c, 5d). Compiled west–east dip angles increase from 10° to 70° over a 30 km seaward distance in the southernmost, Coos Bay, traverse (Figure 5e). These seaward increasing trends of west–east dip angles demonstrate inelastic strain in the upper plate that is associated with convergent plate motions during late Neogene time.

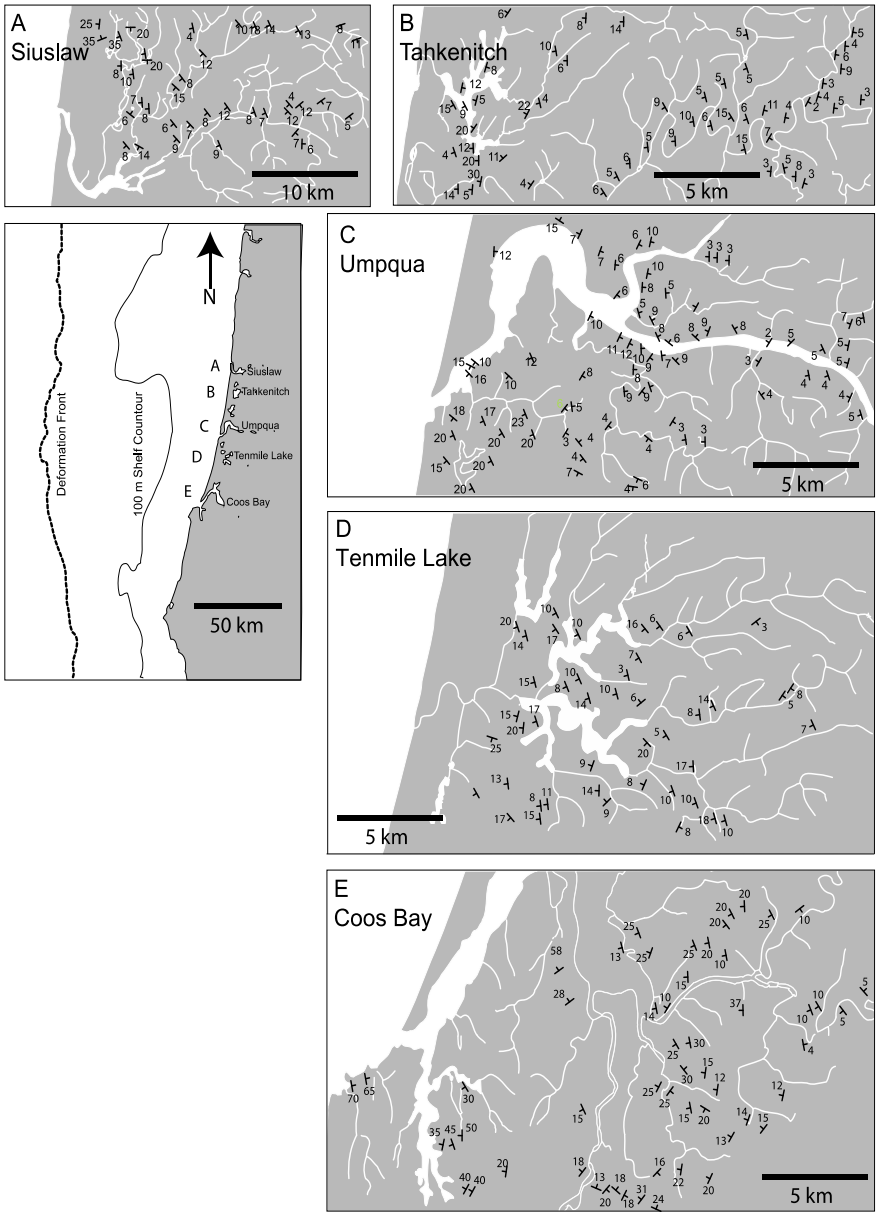

Figure 5. Five coastal drainage traverses showing west–east dip angles of Miocene–Eocene sedimentary rock strata. Siuslaw (A), Tahkenitch (B), Umpqua (C), Ten Mile (D), and Coos Bay (E). Reported dips within 45° of west or east are compiled to represent north–south trending folds or faults at about 1–25 km from the coastline.

Late Pleistocene Strain Records

Uplifted marine and fluvial terraces in the central Cascadia margin have been mapped to investigate possible regional tectonic deformation [West and McCrumb, 1988], local fault offsets [Kelsey, 1990; McInelly and Kelsey, 1990], and/or upper plate segment boundaries

[McNeil, et al., 1998; Personius, 1995]. However, few active faults have been formally established at the surface, suggesting that the topographic deformation is largely associated with subsurface structures. In this chapter the along coast length scales of deformation are used to differentiate regional uplift at hundreds of kilometers in along coast distance from localized terrace warping at tens of kilometers in along coast distance.

Table 2. Elevations of the lowest marine terrace deposits from exposed sections measured in sea cliffs and bay cliffs in the central Cascadia margin

Measured Section	UTM (North)	Elevation (m MSL)	Deformation. Front (km)	Modern Setting	Deposit Sequence	Sec. Ref	Age
Copper Point	5159000	15	148	BC	Ls/TF	1	~80 (2)
Ramsey Point	5157000	10	146	BC	Ls/TF	1	
Pickernell	5156000	7	145	BC	Ls/TF	1	
Long Beach	5134000	8	133	HSC	Ls/TF	-	
Indian Beach	5087000	13	118	SC	Col/Lg	2	
Cannon B.	5080000	11	119	SC	Col/Lg	2	
Arcadia	5077000	8	119	SC	Col/Lg	2	
Hug Point	5075000	13	119	SC	Col/Lg	2	
Arch Cape	5074000	6	119	SC	Col/Lg	2	
Cove Beach	5071000	11	118	SC	Col/Lg	2	
Short Sand	5067000	8	117	SC	Col/Lg	2	
Rockaway	5050000	9	115	HSC	Col/Lg	-	
Garibaldi	5041000	15	116	BC	Ls/Lg	-	
Tillamook	5039000	7	118	BC	Ls/Lg	-	
Cape Mears	5038000	11	114	SC	Co/Lg	2	
Happy Camp	5032000	12	112	SC	Co/BB	4	
Hanson	5030000	10	113	BC	Ls/Lg	2	
Fish	5027000	13	114	BC	Co/Lg	2	
Niflis	5027000	12	114	BC	Co/Lg	2	
Cape Lookout	5023000	9	112	SC	Co/BB	2	
Scout Camp	5017000	8	114	SC	Dn/BB	4	
ATV	5017000	10	114	SC	Dn/BB	4	
Sand Lake	5015000	3	114	BC	Dn/Lg	4	~80 (4)
N. Kiwanda	5009000	4	113	SC	Dn/BB	4	
S. Kiwanda	5008000	10	112	SC	Dn/Pf	4	
N. Daley Lk	4998000	7	110	HSC	Co/Lg	5	
Roads End	4984000	6	112	SC	Dn/BB	5	
21st	4981000	4	112	SC	Dn/BB	4	
Canyon C.	4978000	5	112	SC	Dn/BB	4	
Spahish Head	4976000	5	112	SC	Dn/BB	4	
Glen Eden	4970000	4	111	SC	Dn/BB	4	
Fogerty	4966000	10	106	SC	Dn/BB	5	
Depoe	4965000	13	107	SC	Dn/BB	4	
Boiler Bay	4964000	15	102	SC	Dn/Pf	5	
Otter Rock	4955000	19	101	SC	Dn/BB	5	
Beverly B.	4953000	28	101	SC	Dn/BB	4	
Wade	4951000	24	101	SC	Dn/BB	4	
S. Yaquina	4947000	16	101	SC	Dn/BB	5	

Measured Section	UTM (North)	Elevation (m MSL)	Deformation. Front (km)	Modern Setting	Deposit Sequence	Sec. Ref	Age
Nye Beach	4943000	10	100	SC	Dn/Pf	4	
Newport	4944000	17	100	BC	Dn/Lg	9	~80 (2)
LightHouse	4942000	11	100	SC	Dn/BB	4	
Henderson	4938000	16	99	SC	Dn/BB	4	
Grant Creek	4937000	8	99	SC	Dn/BB	4	
N.Beaver	4931000	6	98	SC	Dn/BB	4	
S. Ona	4929000	4	99	SC	Dn/Pf	4	
Seal Rocks	4927000	7	99	SC	Dn/BB	4	111 (4)
Quail St.	4926000	4	99	SC	Dn/BB	4	
Driftwood	4924000	5	99	SC	Dn/BB	4	
Brucley Cove	4924000	4	99	SC	Dn/BB	4	
Patterson	4918000	7	98	SC	Dn/BB	5	
N. Yachts	4908000	8	97	SC	Dn/BB	4	
Yachats	4907000	6	97	SC	Dn/BB	4	
S Yachats	4907000	6	96	SC	Dn/BB	4	
S. Neptune	4899000	7	95	SC	Dn/Lg	5	
Washburn	4889000	6	95	SC	Dn/BB	5	
Heceta Head	4889000	4	95	SC	Co/BB	-	
Three Mile	4844000	20	97	SC	Dn/BB	-	
Umpqua	4843000	27	97	BC	Dn/BC	-	
Umpqua	4836000	12	96	BC	Dn/BC	-	
Hauser	4813000	9	90	BC	Dn/BC	-	
Fossil Point	4801000	7	85	BC	Dn/Lg	5	
Bastendorf	4800000	9	82	SC	Dn/BB	5	
Lighthouse	4799000	12	80	SC	Dn/BB	5	~80 (6)
Cape Arago	4795000	35	76	SC	Pf	5	
N. Sacci B.	4792000	36	78	SC	Dn/BB	5	
Whisky Run	4786000	23	76	SC	Dn/BB	4	
Golf Course	4785000	22	75	SC	Dn/BB	4	
Coquille P.	4774000	24	68	SC	Dn/BB	4	
DevilsKitchen	4771000	12	67	SC	Dn/BB	5	
N. New River	4767000	5	66	SC	Dn/BB	5	
S. New River	4763000	6	66	SC	Dn/BB	5	
Floras Lake	4750000	9	60	SC	Dn/BB	5	~80 (7)
Blacklock	4748000	40	59	SC	Dn/BB	5	
Cape Blanco	4744000	57	56	SC	Dn/Pf	5	~80(7,8)
SCapeBlanco	4743000	56	54	SC	Dn/Pf	4	
Port Orford	4733000	24	56	SC	Dn/BB	4	

Settings: Sea Cliff (SC); Bay Cliff (BC). Deposit Sequence: Beach Backshore (BB), Beach Cobble (BC), Colluvium (Co), Dune (Du), Loess (Ls), Lagoon (Lg), Platform (Pl), Tidal Flat (TF). Measured Section and Terrace Age References. Clifton [1994], (2) Kennedy, et al. [1982], (3) Mulder [1992], (4) Peterson, et al. [2006], (5) Peterson, et al. [1994], (6) McInelly and Kelsey [1990], (7) Muhs, et al. [1990], (8) Kelsey [1990], and (9) Ticknor [1993]. The sea cliff and bay cliff sections shown here were measured by tape and/or EDM total station and were surveyed to timed mid-swash position (within about ± 0.5 m MSL) [Peterson, et al., 1994; Peterson, et al., 2006].

Most of the marine terraces in the South Central Cascadia Margin are overlain by Pleistocene dune and loess deposits, which are truncated by broad deflation surfaces

[Peterson et al., 2006]. This mantling of the uplifted terraces by dune sheet deposits, up to 30 m in thickness, was unknown to West and McCrumb [1988] at the time of their mapping. The eolian deposits post date the terrace ages by tens of thousands of years [Peterson et al., 2007]. The dune sheets mantle the terraces, filling in valleys and building ramps over buried terrace risers. Some of the broad dune deflation surfaces have been previously misidentified as marine terrace topographic surfaces.

In this chapter the elevations of beach and lagoon deposits that are exposed in modern sea cliffs (Table 2) are used to represent the sea level high stand datum at 80 ka (oxygen isotope stage 5a). The uplifted terraces are dated in key localities by aminostratigraphy [Kennedy et al., 1982], uranium series [Muhs et al., 1990], and thermal luminescence [Peterson et al., 2007] (Table 2).

The use of sea cliff sections to measure terrace height slightly underestimates maximum high-stand elevations taken at platform backedges [Bradley and Griggs, 1976] but this method yields a consistent terrace elevation proxy along this straight narrow coastal plain. Where long-term uplift rates are low, the 80 ka terrace might reoccupy previous high stand platforms at 105 ka (stage 5c) and/or 120 ka (stage 5e). In any case the lowest preserved high stand beach or lagoon deposit is used to establish vertical deformation of the latest Pleistocene marine terrace datum.

The high stand deposits exposed in bay cliffs and sea cliffs in the northern part of the study area consist of lagoon or bay wetland mud [Mulder, 1992**;** Clifton**,** 1994], representing elevations of 0–2 m above the 80 ka paleosea level datum. The majority of marine high stand deposits that are exposed in sea cliffs along the central and southern parts of the study area consist of beach backshore sand. Modern backshore sand deposits reach 4–5 m above mean sea level in the study area [Peterson et al., 1994], but the regressive deposits exposed in the sea cliffs likely reflect slightly lower elevations, thereby yielding elevations that are probably 1–3 m above the 80 ka paleosea level datum.

The bay cliff and sea cliff sections provide abundant exposures of the lowest marine terrace (76 sites recorded), except where covered by the thick dune sheets between the Siuslaw and Coos Bay drainages, (4820000-4880000 UTM-N; Table 2). Elevations of the upper contact of the lagoon or beach high stand deposits at 80 ka are measured by leveling to predicted tidal level (± 0.5m). The measured eleavations are corrected to mean sea level (MSL) which is about 1.0 m above the regional 0 m NAVD88 datum in the study area.

A plot of terrace elevations along the South Central Cascadia Margin shows increasing modern elevations of the 80 ka high stand deposits from Willapa Bay (~10 m MSL) to Cape Blanco (57 m MSL) at the Elk drainage (Figures 3 and 6).

The coastal record of late Pleistocene marine terrace deformation is extended slightly beyond the limits of the South Central Cascadia Margin (Figure 1) to identify any terrace warping trends (tens of kilometers length scale) at the ends of the study area. The densely sampled terrace sections show increasing variability of the 80 ka deposit elevations with increasing distance south along the study area coastline (Figure 6). In the northern bay and sea cliffs the 80 ka high stand deposits range from about 5 to 15 m elevation. In the southern sea cliff exposures the 80 ka high stand deposits range from 5 to at least 35 m elevation. Broadly even regional uplift in the northern coastline transitions to local warping in the south coast. The late Pleistocene terrace warping is likely associated with folds and/or underlying faults that obliquely intersect the coast (Figure 3) in the southern part of the study area.

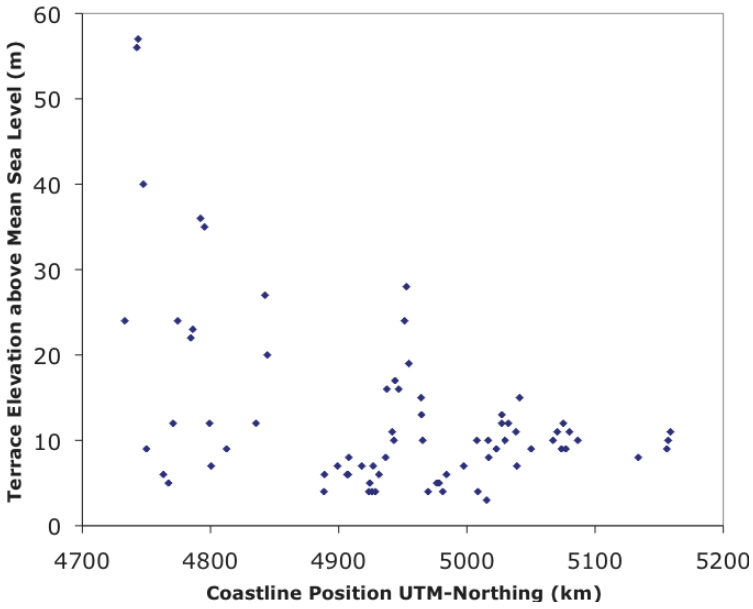

Figure 6. Plot of marine high-stand deposit elevations versus position in the central Cascadia margin from measured sections in sea cliffs and bay cliffs (see Table 2 for measured section data). Cape Blanco (~ 4740 km UTM) is located at the Elk River drainage, and Willapa Bay (~ 5150–5160 km UTM) is located just north of the Columbia River mouth (Figure 2).

Late Holocene Strain Records

Episodic coastal subsidence as recorded in late Holocene tidal wetland deposits has been documented in many estuarine sites in the South Central Cascadia Margin [Darienzo, 1991; Nelson, 1992; Darienzo et al., 1994; Witter et al., 2003, among others]. Paleotidal level datums recorded by plant macrofossils and microfossils are used to establish episodic events of land level submergence or emergence, which are superimposed over longer-term trends of net sea level rise in the South Central Cascadia Margin [Darienzo and Peterson, 1990]. In this chapter selected core site records are compiled from estuaries with the greatest landward extent of tidal influence in the study area. Significant tidal influence in the lower Columbia River estuary extends over 100 km landward from the coastline, a distance sufficient to establish the limit of recorded subsidence at site CRLV2, located at Longview, Washington (Figure 7).

The wetland subsidence records are based on downcore changes in plant macrofossil type and abundance, as detailed elsewhere [Barnett, 1997; Peterson et al., 2000]. In short, the amounts of abrupt paleosubsidence (0-2 m vertical subsidence) are based on abrupt upcore decreases in peat content and/or tree roots, which reflect vegetated wetland burial by intertidal mud. Two of these authors were the first to use microfossil paleosalinity indicators, including diatoms and foraminifera, to confirm abrupt subsidence records in Netarts Bay (Figure 8) [Darienzo, 1987; Darienzo and Peterson, 1990]. Other investigators subsequently used these salinity indicators in Cascadia Margin wetlands [Briggs, 1994; Nelson et al., 1996; Atwater and Hemphill-Haley, 1996**;** Barnett, 1997] to show freshwater wetlands submerged and then buried under saline intertidal mud. However, salinity wedges in the fluvially dominated

estuaries in the South Central Cascadia Margin only reach about one third of the landward distance of tidal influence. The geographical limitations of salinity indicators greatly bias or reduce the spatial distribution of paleosubsidence records that are recorded in fluvially dominated estuaries in the South Central Cascadia Margin.

In this chapter the macrofossil records of vegetated wetland burial are used to establish three conditions of episodic subsidence, including 0 ± 0.5 m, 1 ± 0.5 m, and 1.5 m ± 0.5 m subsidence. At least two abrupt subsidence events that occurred during the past 2,500 years are used to establish the maximum amounts of cyclic abrupt subsidence in a core site. An interpretation of abrupt subsidence is based on sharp upper contacts (< 1cm width) between the subsided wetland and the overlying bay mud. With the exception of some new core site data from the Columbia and Coquille estuaries (Figure 2) the core site coordinates, subsidence records, and radiocarbon dates used for this study have been previously reported [Briggs, 1994; Barnett, 1997; Petersen et al., 2007]. For this study the core records are compiled from west to east traverses in estuaries with tidal reaches that extend at least 10 km inland from the coast in the South Central Cascadia Margin. These estuaries include the Columbia, Netarts and Tillamook Bays, Siuslaw, Umpqua, Coos, and Coquille (Figure 2).

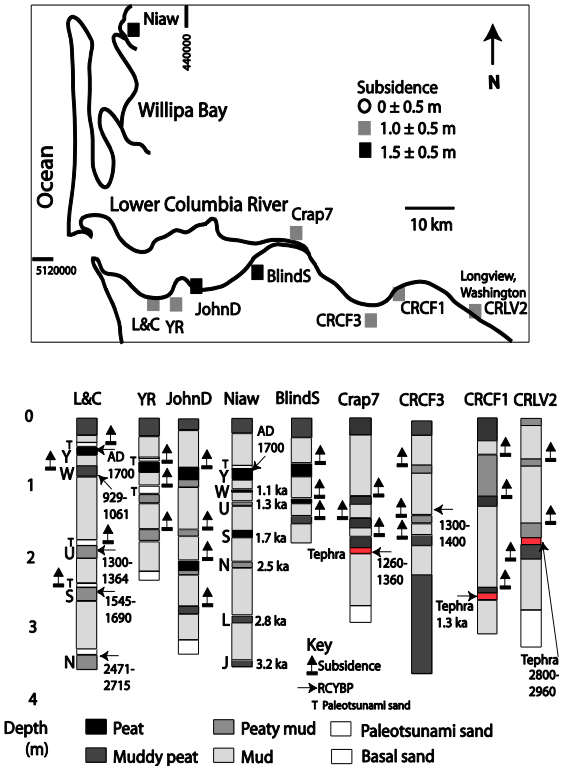

Figure 7. Map of core sites and selected core logs for the Lower Columbia River and Willapa Bay. Several abrupt submergence events in the lower reaches of the Columbia River estuary including core sites LandC and YR are associated with paleotsunami sand layers. Coseismic subsidence events in site LandC are correlated to subsidence events in Willapa Bay at site Niaw (Niawiakum) (Atwater and Hemphill-Haley, 1996; Atwater et al., 2004). The greatest amounts of subsidence (1.5 m) in the lower Columbia River occur between John Day Creek (JohnD) and Blind Slough (BlindS). This position corresponds to the trough of maximum coseismic subsidence (~ 1.5 m subsidence), located 30–40 km landward of the river mouth.

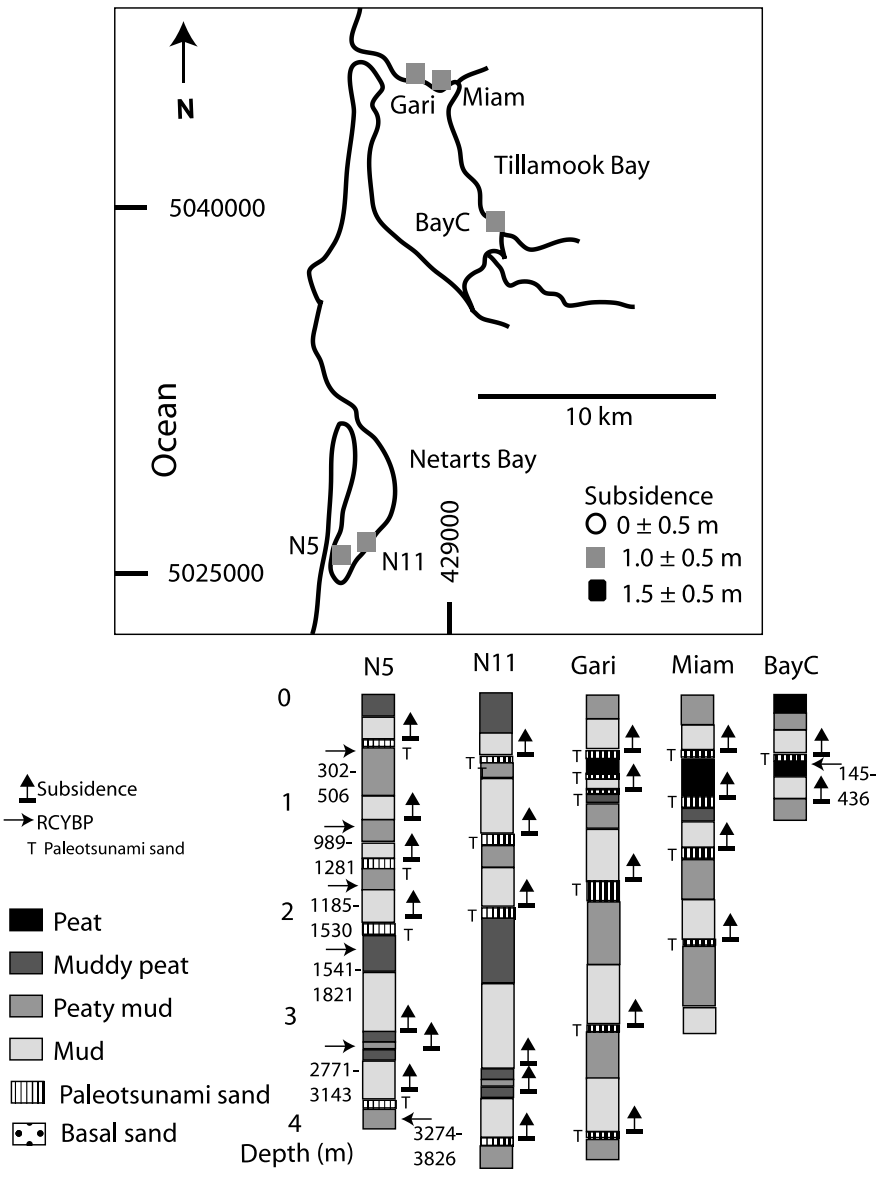

Figure 8. Map of core sites and selected core logs for the Netarts and Tillamook Bays. Abrupt wetland subsidence events are associated with paleotsunami sand layers showing correlation to regional megathrust ruptures in the Cascadia Margin. Seven subsidence events are recorded during the last ~ 3,200 years in Netarts Bay, demonstrating a mean recurrence interval of 430 years. Subsidence events in Netarts Bay are estimated to generally range from 0.5 to 1.0 m in abrupt submergence, though the last subsidence event in Tillamook Bay might reach 1.5 m.

Radiocarbon dates published by Jurney [2001] and Witter et al. [2003] in the lower Columbia and Coquille estuaries, respectively, are used to augment core logs collected in those localities by the authors of this chapter. One core log (Niaw) from the eastern margin of the tidally dominated Willapa Bay [Atwater and Hemphill-Haley, 1996] is presented for comparison to the fluvially dominated reaches of the lower Columbia River (Figure 7).

Table 3. Radiocarbon ages of selected core site intervals from South Central Cascadia Margin tidal basins

Core Site Depth (cm)	Conventional Age RCYBP	Calibrated 1s Age RCYBP	Calibrated 2s Age RCYBP	Beta Analytic, other ()Lab ID
CRCF3 (125)	1470 ± 30	1330 – 1380	1300 – 1400	294493
CRAP7 (180)	1380 ± 50	1280 – 1320	1260 – 1360	294489
LandC (60)	1080 ± 40	937 - 1052	929 - 1061	121421
LandC (180)	1438 ± 19	1309 – 1341	1300 – 1364	(UB)4499
LandC (240)	1698 ± 15	1562 – 1682	1545 – 1690	(QL)4922
LandC (340)	2488 ± 21	2494 – 2705	2471 – 2715	(UB)4497
CRLV2	2450 ± 30	2365-2691	2360– 2710	304399
BayC (55)	250 ± 50	150 – 427	141 - 464	89165
N5/11 (56)	350 ± 60	318 – 480	302 -506	24933
N5/11 (114)	1220 ± 60	1060 – 1239	989 – 1281	24934
N5/11 (190)	1450 ± 80	1287 – 1413	1185 – 1530	24935
N5/11 (220)	1760 ± 60	1569 – 1766	1541 – 1821	24521
N5/11 (360)	2820 ± 70	2846 – 3036	2771 – 3143	25030
N5/11 (420)	3290 ± 100	3405 – 3635	3274 – 3826	24523
S 216 (127)	1320 ± 60	1180 - 1298	1084 - 1338	67450
S 216 (153)	1540 ± 70	1373 - 1518	1303 - 1560	58117
S 216 (167)	1450 ± 70	1296 - 1400	1271 - 1519	67451
S 216 (210)	1910 ± 70	1739 - 1930	1634 - 2033	58118
S 222 (40)	30 ± 90	modern		58119
S 222 (322)	1910 ± 70	1739 - 1930	1634 - 2033	58120
U 301 (78)	400 ± 60	329 - 512	314 - 523	67455
U 301 (290)	2530 ± 80	2489 - 2746	2362 - 2755	67456
U 321 (205)	1420 ± 80	1277 - 1403	1179 - 1517	67460
U 328 (255)	2450 ± 70	2362 - 2697	2353 - 2716	58121
U 332 (76)	1270 ± 90	1088 - 1287	980 - 1331	58122
U 332 (130)	2820 ± 70	2846 - 3060	2771 - 3143	58123
U 332 (180)	2960 ± 60	3005 - 3239	2957 - 3330	58124
U 337 (260)	2150 ± 80	2008 - 2305	1950 - 2337	67458
U 337 (375)	3140 ± 70	3266 - 3446	3164 - 3555	67459
U 339 (89)	1040 ± 60	913 - 1054	794 - 1067	58125
U 339 (179)	1630 ± 60	1416 - 1596	1390 - 1693	58126
U 339 (225)	1850 ± 60	1715 - 1864	1619 - 1924	58127
JNEY (45)	400 ± 50	342 -532	319 -544	110469
JNEY (86)	1080 ± 60	986 – 1170	956 – 1256	110470
C 408 (80)	650 ± 70	557 - 669	525 - 696	27675
C 408 (232)	2350 ± 90	2184 - 2685	2153 - 2712	27743
C 408 (329)	2760 ± 80	2778 - 2945	2744 - 3074	34278
C 408 (550)	3620 ± 160	3707 - 4149	3561 - 4413	34279
C 448 (75)	1800 ± 60	1628 - 1819	1569 - 1869	58137
C 448 (205)	2830 ± 100	2797 - 3076	2754 - 3238	58138
C 449 (65)	1000 ± 50	800 - 963	788 - 1501	58134
C 449 (98)	1390 ± 60	1269 - 1354	1179 - 1404	58135
C 449 (139)	1780 ± 60	1619 - 1811	1553 - 1862	58136
C 465 (68)	1970 ± 70	1827 - 1996	1737 - 2113	58128
C 465 (95)	3080 ± 60	3161 - 3398	2994 - 3479	58129
C 465 (420)	4560 ± 70	5054 - 5437	4976 - 5465	58130
C 470 (72)	1020 ± 70	799 - 1051	744 - 1070	67437
C 470 (121)	1400 ± 80	1192 - 1393	1150 - 1517	67438
C 470 (190)	1660 ± 80	1419 - 1692	1373 - 1774	67439
C 470 (250)	2900 ± 80	2929 - 3202	2848 - 3321	67440
C 470 (305)	3700 ± 90	3901 - 4154	3777 - 4402	58133

Core Site Depth (cm)	Conventional Age RCYBP	Calibrated 1s Age RCYBP	Calibrated 2s Age RCYBP	Beta Analytic, other ()Lab ID
C 476 (115)	1780 ± 90	1574 - 1819	1446 - 1923	67441
C 476 (210)	1930 ± 70	1815 - 1987	1707 - 2042	58139
C 478 (140)	1740 ± 100	1539 - 1810	1415 - 1872	67443
C 478 (395)	2920 ± 60	2970 - 3161	2882 - 3257	67444
FAHY (77)	240 ± 40	150 -420	143-430	221465
Coquille521 (245)	2430±40	2360 - 2680	2350 – 2710	305787
Elk/A2 (295)	2980 ± 60	3069 – 3262	2977 – 3339	73248

Dates from Columbia River (LandC) [Journey, 2001], Columbia River (CR) (this chapter), Tillamook Bay (BayC) [Barnett, 1997], Netarts Bay (N) [Darienzo and Peterson, 1990]. Siulsaw (S), Umpqua (U) and Coos Bay (C) [Briggs, 1994; Barnett, 1997; Peterson et al., 1997], Coquille (FAHY) (this chapter), and Elk (this chapter). Radiocarbon date calibration (Siuslaw, Umpqua, Coos) (CALIB 5.02. Stuiver, et al., 2005) and all other dates (CALIB 6.02. Stuiver, et al., 2011). See Figures 7–12 for core site positions and lithologic logs.

One dated core section from the Elk River estuary, located just south of the study area (Figure 1) is presented here for the first time to compare to more extensive work in the adjacent Sixes estuary reported by Kelsey et al [2002]. Radiocarbon data for all of the late Holocene wetland sites shown here are presented in Table 3.

The core logs that are shown in this chapter are generally taken from continuous vibracores or pound cores (7.5 cm diameter) that were split, photographed, logged, and subsampled under laboratory conditions. Plant macrofossil type and relative abundance are based on standardized observation and on loss on ignition, respectively, as detailed elsewhere [Darienzo, 1991; Barnett, 1997]. Diatoms are used to confirm paleosubsidence estimates based on peat content and/or presence of tree roots in the lower saline reaches of the estuaries. Diatom data are presented elsewhere for Netarts [Darienzo, 1991], Tillamook [Barnett, 1997], Siuslaw, Umpqua, Coos [Briggs, 1994], and Coquille [Witter et al., 2003]. In this chapter the plant macrofossils are used to extend the paleosubsidence records well landward of the ocean coastline in freshwater tidal reaches of the estuaries. For example, both the numbers of events and amounts of recorded paleosubsidence increase with increasing distance from the coast in the Siuslaw estuary, with at least 3–4 events recorded near Mapleton, Oregon (Figure 9).

In this chapter the presence of tree roots or peat (>50% organic content) are used to designate paleotidal elevations of at least 1.5 m paleomean sea level (pMSL). Barren mud or slightly rooted mud occur at 0 m pMSL in the study area estuaries [Darienzo and Peterson, 1990; Barnett, 1997]. Muddy peat at 1.0 m pMSL and peaty mud at 0.5-0.75 m pMSL represent intermediate paleotidal level indicators. Upcore abrupt transitions between these four different paleotidal indicators indicate the amount of submergence (0 ± 0.5 m, 1.0 ± 0.5 m, and 1.5 ± 0.5 m) used in this chapter. Most importantly peat or tree root to mud transitions represent 1.5 m of submergence. Core sections lacking transitions between any two of the other indicators represent 0 m or no episodic submergence within the detection limits of the plant macrofossils. For example, the general absences of two or more recorded subsidence events are well established in the lowermost reaches of the Umpqua River estuary in the central part of the study area (Figure 10).

Radiocarbon ages of peat samples provide loose constraints on core depth age and recorded event recurrence intervals during the inferred subsidence events (Table 3). Event correlations based on deposit radiocarbon ages are problematic in the southern part of the study area due to the modest and spatially variable aspects of the subsidence events.

Paleotsunami inundations, as established by landward thinning sand sheets at paleosubsidence contacts, provide much better correlations of local subsidence to regional megathrust ruptures, such as in the South Slough syncline (sites JNEY and 408) in the lower reaches of Coos Bay (Figure 11).

West–east core traverses in the south central part of the study area demonstrate increasing numbers of subsidence events with distance landward from the coast in the Siuslaw and Umpqua estuaries (Figures 9 and 10). The most striking example of increasing episodic coastal subsidence with increasing distance landward of the coast occurs in the Coquille estuary. The core sites 521–523 at Coquille, Oregon, contains twice the number of subsidence events for the same depth interval as the core sites FAHY and 504/503 in the lower reaches of the Coquille estuary (Figure 12).

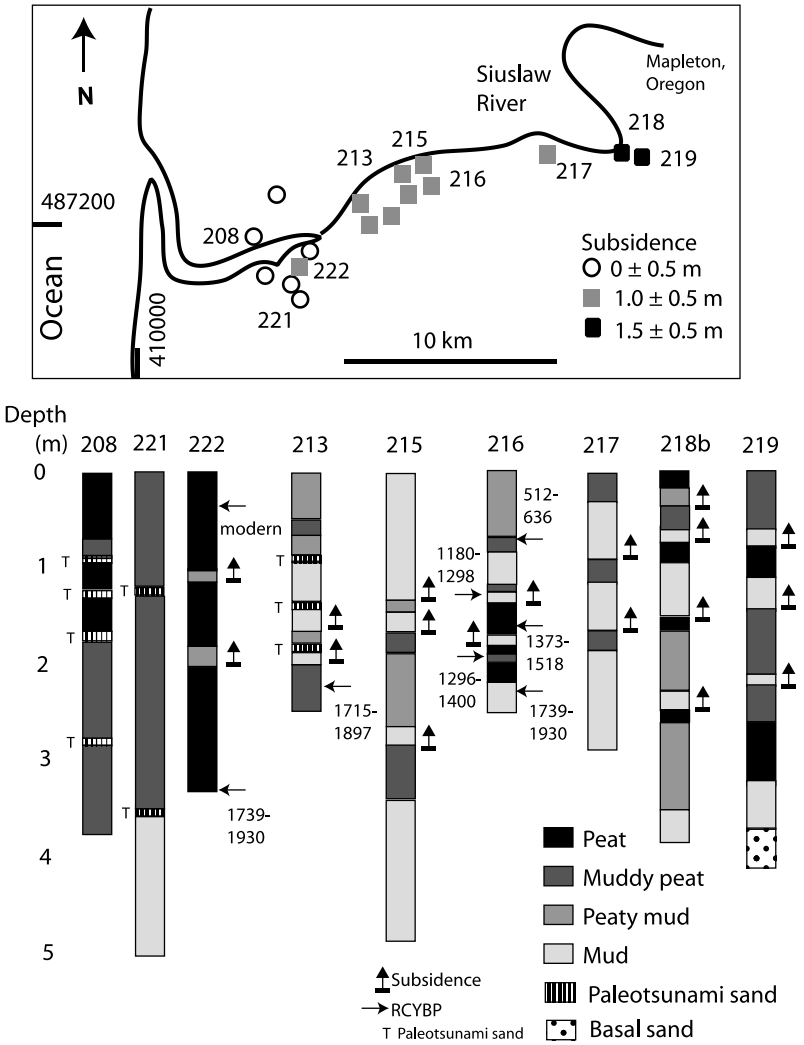

Figure 9. Map of core sites and selected core logs for the Siuslaw River estuary. Abrupt wetland subsidence events increase in number and in relative submergence with distance landward (25 km) from the coast. Three to five subsidence events are recorded during the last 1700–1900 years in the upper reaches of the Siuslaw estuary.

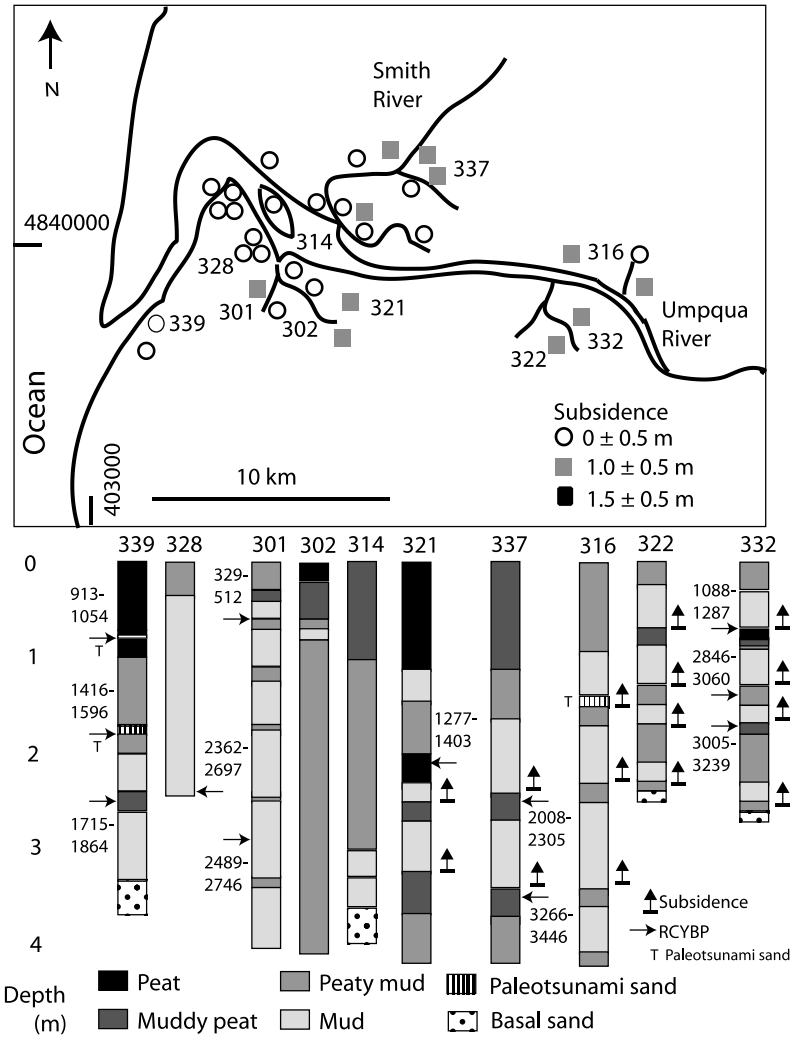

Figure 10. Map of core sites and selected core logs for the Umpqua River estuary. Abrupt wetland subsidence events increase in number with distance landward (20 km) from the coast. Four subsidence events are recorded during the last ~ 3,500 years in the upper reaches of the Umpqua estuary. A thick paleotsunami sand sheet overlies a dated peat (1416–1596 BP) at site 339 near the mouth of the estuary. An undated paleotsunami deposit is recorded at river bank site 316, located nearly 30 river kilometers from the tidal inlet.

One representative core log (Elk/2A) is shown for the Elk River tidal wetlands at Cape Blanco (Figure 12). The Elk River Drainage is located in the South Cascadia Margin, landward of the Gorda Plate segment (Figure 1). It is discussed briefly in this chapter due to its proximity to the Coquille estuary, at the south end of the South Central Cascadia Margin. The paleosubsidence records in the Elk River wetlands are very weak, with subsidence amounts at or below the threshold of detection (<0.5 m abrupt submergence).

By comparison, Kelsey et al., [2002] report substantial amounts of episodic subsidence in the nearby Sixes River wetlands. It is not presently known whether the greater subsidence estimates in the Sixes River wetlands could be influenced by paleotsunami input of marine/brackish diatoms or whether the larger subsidence values reflect anomalous stain

associated with an upper plate structure, as suggested by Kelsey et al., [2002]. Locally enhanced episodic subsidence has been established in the South Slough and Pony Slough synclines of Coos Bay (Figure 11). The focus of the elastic strain investigations reported in this chapter are at the regional scale rather than the local scale, so the localized subsidence records in the lower reaches of the southern estuaries are not further discussed here.

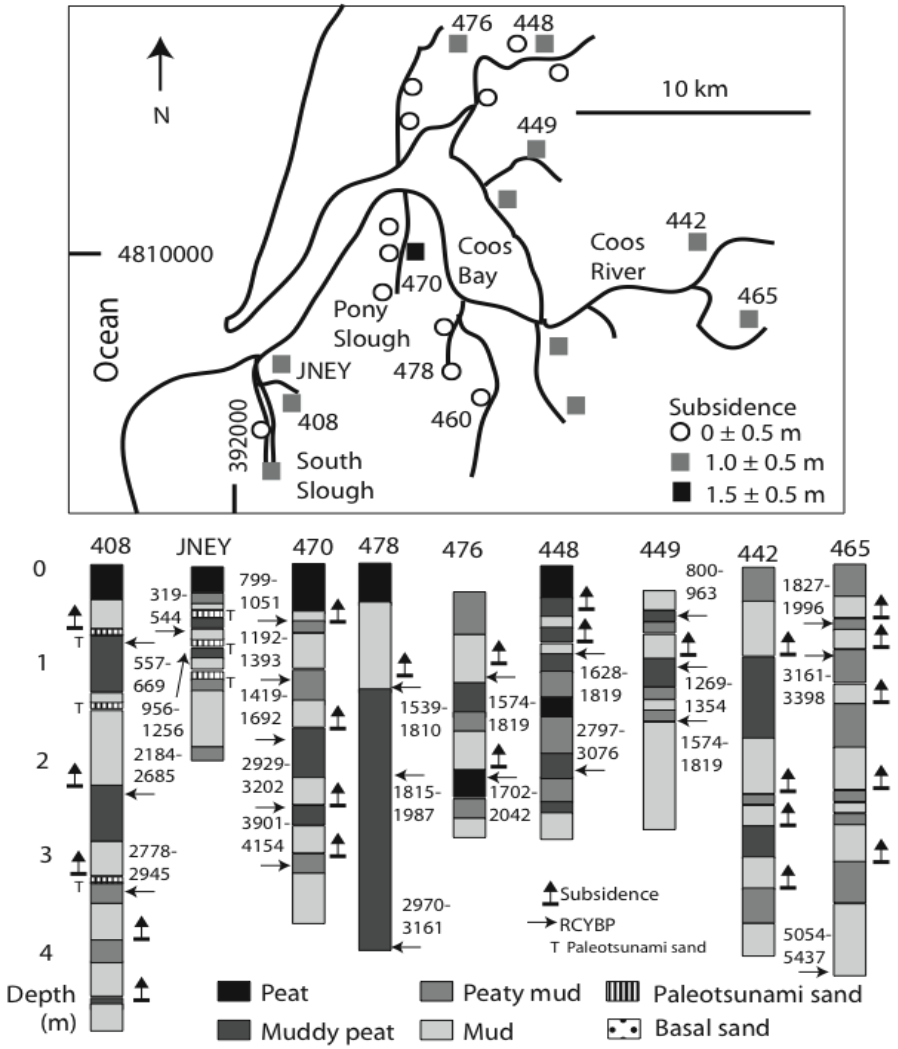

Figure 11. Map of core sites and selected core logs for the Coos Bay and South Slough estuaries. The distribution of recorded subsidence events in Coos Bay is complex, with modest subsidence events (1.0 ± 0.5 m) or no subsidence (0 ± 0.5 m) in core sites that are comingled between distances of 5 and 25 km from the coast. However, episodic subsidence is locally enhanced in mapped fold axes in South Slough and Pony Slough [Newton, 1980]. Paleotsunami inundation is recorded with at least 3 of 5 abrupt subsidence events in sites JNEY and 408 near the Coos Bay tidal inlet, showing the localized subsidence to be correlated to regional megathrust ruptures.

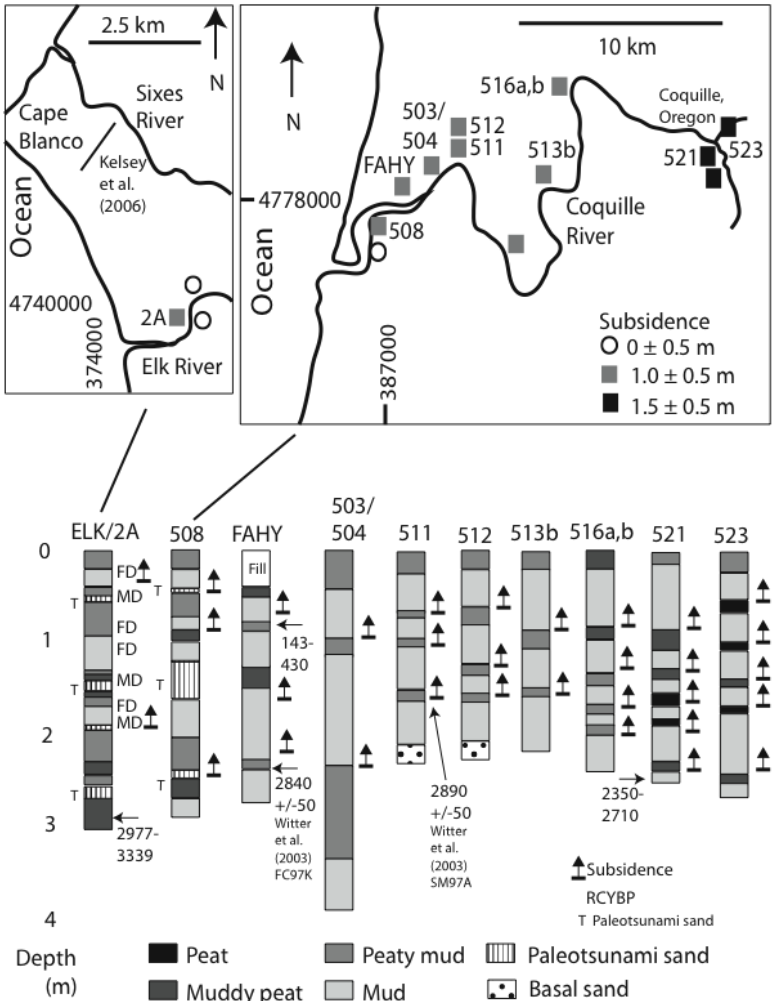

Figure 12. Map of core sites and selected core logs for the Coquille estuary and Elk River wetlands. Abrupt wetland subsidence events in the Coquille estuary increase in number and in relative submergence with distance landward (20 km) from the coast. Two events approaching or reaching 1.5 m are recorded in the most landward sites 521–523. Un-calibrated basal radiocarbon dates, which are used to estimate section ages in sites FAHY and 511, are from nearest core sites, FC97K and SM97A respectively, as reported by Witter et al., [2003]. The record of subsidence in the Elk River estuary is weak. Marine diatoms (MD) likely associated with paleotsunami inundations interrupt the otherwise freshwater diatom assemblages (FD) in the small Elk River wetlands at site Elk/2A. Kelsey et al. [2002] have reported records of episodic subsidence in core sites located in a traverse in the nearby Sixes River (solid line).

DISCUSSION

Late Neogene Coastal Deformation

Long-term convergent deformation in the Cascadia margin is reflected, in part, by north trending folds and/or monoclines associated with west-east compression of the upper plate. Compiled west- and east-dip angles of coastal Tertiary formations in the south-central

Cascadia margin decrease with distance landward of the coastline (Figure 5). A plot of those bedding dip angles versus their landward distance from the deformation front or buried trench at equivalent latitudes is shown in Figure 13.

A regional dip angle of 3° to 6° to the west occurs at landward distances of at least 120 km from the deformation front in the central part of the study area (Figure 13). The regional dip is associated with Neogene uplift of the Coast Range. Larger dip angles of 10° to 20°, and 20° to 30° respectively, are mapped at distances of 110 and 100 km from the deformation front. The seaward increase in dip angles of the Tertiary strata indicate long–term convergent strain accumulation, associated with interplate coupling of the Cascadia megathrust, at distances of up to 110 km from the deformation front in the South Central Cascadia Margin. The inelastic deformation could either reflect overlying plate compression from an underlying strongly coupled zone and/or deformation propagated a short distance landward of the strongly coupled zone in the upper plate. The duration and/or frequency of strain accumulation during the late Neogene are not addressed here, but Quaternary records of inelastic strain are provided by late Pleistocene uplift and warping of marine terraces (see below).

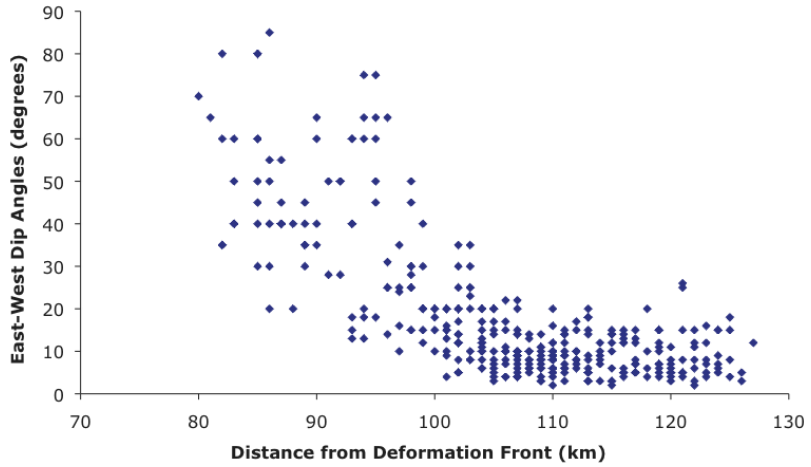

Figure 13. Tertiary strata dip angles as a function of across margin distance to the deformation front or buried trench. Graphed data are from Figure 5.

Late Pleistocene Coastal Deformation

The along coast variability in the elevations of the uplifted 80 ka marine terrace(s) serves as a proxy for inelastic upper plate deformation in the central Cascadia margin during the late Quaternary. In this chapter the regional scale of coastal terrace uplift, possibly related to broad under plating or other deeper processes, is discriminated from local terrace warping. The local vertical warping is assumed to be associated with compression in upper plate structures such as folds and/or underlying faults. The relative uplifts of the marine terraces are based on the elevations of 80 ka high-stand deposits, as measured in bay cliff and beach cliff exposures (Table 2).

A vertical deformation index aids in visualizing the heights of the 80 ka high stand deposits binned at approximately 50 kilometer intervals along the coast in the study area (Table 4). Two 50 km intervals are combined in the central part of the study area where the late Pleistocene dune sheet cover is most extensive. Terrace elevation data is summed and averaged for each 50 km interval to calculate mean elevation and standard deviation from the mean. The standard deviation does not represent error about the mean, but instead it represents the square of the measured elevation variance (see further discussion below).

Table 4. Grouped elevation data for lowest marine terrace in along coast intervals from the South Central Cascadia Margin

Along coast Interval UTM-N	Average Position (UTM-N)	Trench Distance (km)	Average Elevation (m)	Standard Deviation (± m 1s)
5159000-5146000	5146000	142	10.0	3.5
5086000-5067000	5076000	119	10.3	3.0
5050000-5008000	5029000	110	9.5	3.4
5008000-4964000	4986000	108	8.0	4.0
4955000-4918000	4936000	101	9.5	3.4
4908000-4812000	4860000	95	10.5	7.4
4800000-4763000	4781000	75	17	11
4750000-4733000	4741000	56	32	23

See Table 2 for lowest terrace elevation Data.

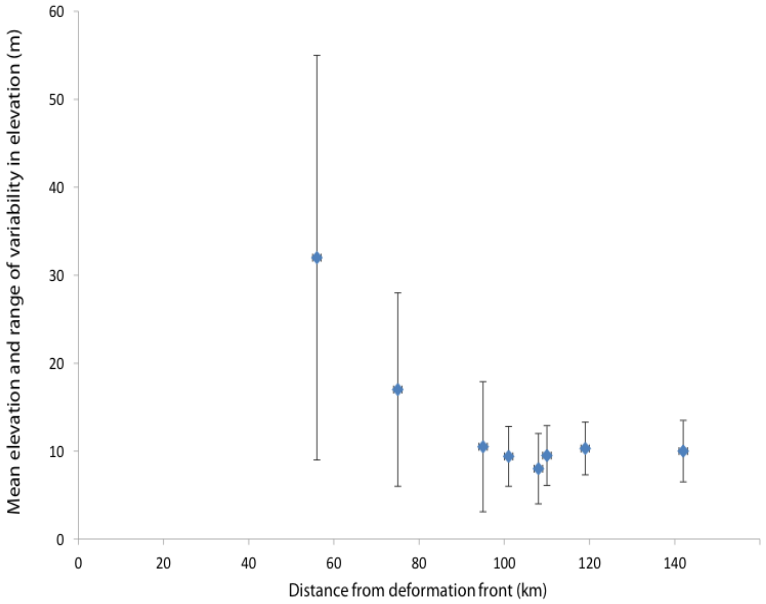

Figure 14. Plot of lowest marine high stand deposit (80–120 ka) elevations including mean and range of variability of elevations in meters (m) NAVD88 for each 50 km alongshore interval (data from Table 2).

The midpoint of each 50 km interval is measured for its distance from the buried trench or deformation front (x-axis in Figure 14). The mean elevation is a simple average of measured sea cliff sections, with no intent to bias sample selection on the basis of terrace height maxima, minima or apparent offsets. The range in elevation variability is taken as the square of elevation variance. It is not an error measurement, but rather a measure of variability of terrace deposit height within each 50 km distance interval (Figure 14).

The ranges of variability of the high stand deposit elevations are shown as ± the square of variance about the mean. The range of elevation variability changes from ± 3–4 m at distances greater than 100 km from the deformation front to ± 10–20 m at 50–70 km distance from the deformation front. The increase in range of variability of terrace elevation reflects broad warping that is likely associated with shore oblique folds and or buried thrust faults in the deformation belt. Localized terrace vertical offsets are not thought to represent plate segmentation or to impact megathrust rupture lengths as has been suggested by other investigators [Kelsey et al., 2002]. However, an increase in the variability of terrace elevations from north to south in the study area is thought to reflect the intersection of the coast with the fold and fault deformation belt. A modest regional uplift of ~ 10 m in the northern coastal terraces occurs landward of the deformation belt. This regional uplift is measured at approximately 10 m per 100,000 years or ~ 0.1 mm yr^{-1}. This regional uplift, possibly reflecting broad underplating in the subduction zone, is differentiated from compressive shortening in the deformation belt. The averaged elevations (~ 30 m) of 80 ka high stand deposits from coastal terraces that occur well within the deformation belt could represent crustal shortening by combined shallow folds, thrusts, and/or more complex structures at depth.

The local terrace warping reaching 80-90 km distance landward of the deformation front in the south central part of the study area is associated with compressive strain in the upper plate. The substantial terrace warping either directly overlies the zone of strong interplate coupling or it extends a very short distance landward of the strongly coupled zone.

Late Holocene Coastal Deformation

Coastal deformation is recorded by alternating interseismic uplift and coseismic subsidence in late Holocene tidal marshes of the South Central Cascadia Margin. One small tidal basin, Netarts Bay, is particularly sensitive to episodic subsidence events in the South Central Cascadia Margin. Two weak subsidence events at 1.3 ka and 2.8 ka were initially found in the Netarts wetlands [Darienzo, 1987; Darienzo and Peterson, 1990] before their subsequent recognition in larger tidal basins [Atwater and Hemphill-Haley, 1996]. The interseismic intervals recorded in Netarts Bay are quite variable, ranging from 200 to 900 years during the last 3.2 ka (Figure 15). The mean recurrence interval for 7 subsidence events in Netarts Bay between 3.2 and 0.3 ka is 430 years. The long–term trends of paleotidal level indicators in Netarts Bay (3.2 ka long record) coincide with eustatic sea level rise of ~ 1.0 m per thousand years. The alternating episodes of interseismic uplift and coseismic subsidence in Netarts Bay are fully elastic.

The ranges of interseismic uplift values are well constrained by the paleotidal level indicators in Netarts Bay, as uplift does not reach supratidal elevations. Maximum uplift ranges between 0.75 and 1.25 m pMSL (Figure 15). A problem exists with regards to the

apparent rates of interseismic uplift between subsidence events in Netarts Bay. The longer interseismic intervals (>500 years) do not reflect the total gain in paleotidal elevation that would be expected from the higher rates of uplift demonstrated by the shorter interseismic cycles and the present interseismic cycle (0.3 ka to the present). It is not known whether 1) lower strain rates lead to longer recurrence intervals or 2) whether early rates of uplift are followed by decreasing rates of vertical strain prior to megathrust rupture. These questions relate directly to predictions of the timing of the next great earthquake in the study area. Will the next great earthquake follow a short strain cycle or long strain cycle? Will a change in modern strain rates (Figure 4) signify a precursor to the next megathrust rupture?

In the southern part of the study area the locally enhanced subsidence, such as in South Slough, Coos Bay (Figure 11) is possibly related to upper plate structures (Figure 3). It is not known to what degree the localized strain is elastic, or whether the localized strain reflects stress release or stress accumulation during the megathust ruptures. Such localities of locally enhanced strain, including the Sixes River wetlands (Figures 11 and 12) deserve further investigations, by seismic profiling, to establish the geometry and scale of possible underlying upper plate structures. The focus of this study is on the distribution of regional elastic strain in the upper plate (as discussed below).

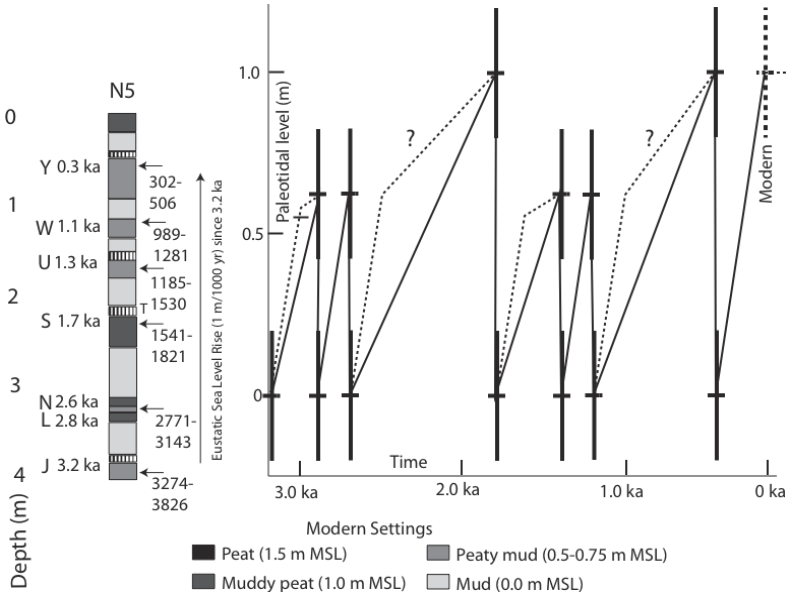

Figure 15. Core log and radiocarbon dates from core site N5 in Netarts Bay (redrafted from Figure 8). Great earthquake designations (letters), and ages (ka), follow those from the Niaw core site in the Niawiakum tidal creek of Willapa Bay (Figure 7) [Atwater and Hemphill-Haley, 1996; Atwater et al., 2004]. Paleotidal levels are shown at the ends of interseismic uplift and coseismic subsidence for each interval in site N5 from Netarts Bay. Two plots of interseismic uplift for Netarts Bay are shown including uplift rates fitted for each earthquake cycle (solid line) and early uplift rates (dashed line) taken from the most recent interseismic uplift (0.3 to 0.0 ka) followed by late uplift rates fitted to the measured paleotidal level datum. The modern marsh elevation has already reached the maximum interseismic uplift that has occurred prior to previous megathrust ruptures. Little or no additional vertical strain accumulation is expected to occur prior to the next megathrust rupture. Data and figure modified from Darienzo and Peterson [1990].

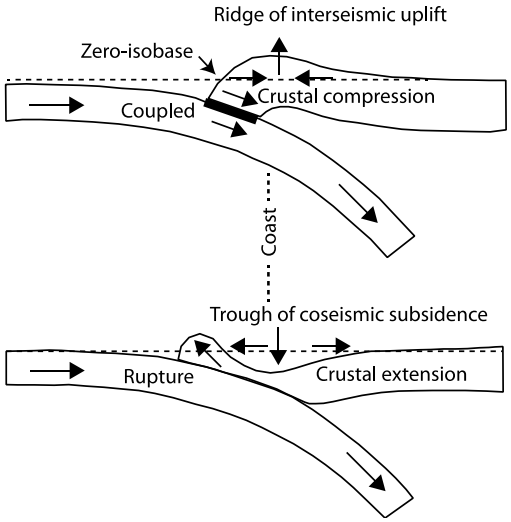

Figure 16. Cross section diagram of interseismic coastal uplift during interplate coupling (upper) and coseismic subsidence during megathrust rupture (lower). Figure is redrafted from several sources. Vertical scales are greatly exaggerated to highlight the trough of coseismic subsidence, reaching a maximum value at the position of the vertical arrow. A zero-isobase occurs between the trough of coseismic subsidence and the seaward area of coseismic uplift. Coseismic subsidence should approach 0 m near the zero-isobase, which approximates the landward extent of the strongly coupled zone.

The regional trough of coseismic subsidence coincides with the ridge of interseismic uplift in the upper plate (Figure 16). A zero-isobase occurs between the trough of coseismic subsidence and the ridge of coseismic uplift.

Coseismic uplift events might be difficult to recognize in wetland settings where plant roots grow or descend well below marsh surfaces. However, the regional zero-isobase should be apparent where mapped subsidence values diminish to zero. Equally important in constraining the geometry of upper plate elastic strain is the trough of maximum coseismic subsidence (see below).

The full width of the trough of coseismic subsidence is contained within the tidal reach of the lower Columbia River (Figure 7). The most landward extents of the last three dated coseismic subsidence events (0.3, 1.1, and 1.3 ka) are observed in site CRCF1, at a distance of 185 km from the deformation front. The greatest landward extent of apparent episodic subsidence in the lower Columbia River at CRLV2 in Longview, Washington, is about 200 km from the deformation front. The trough of maximum coseismic subsidence (1.5 m subsidence) is bracketed between sites JohnD and BlindS, at distances of 145 and 155 km from the deformation front, respectively. These core sites contain at least two recorded subsidence events each of maximum subsidence (~ 1.5 m) based on plant macrofossil indicators of paleotidal level. The lower Columbia River is the only tidal system setting in the South Central Cascadia Margin that spans the full width of the trough of coseismic subsidence.

Coseismic subsidence events in Netarts and Tillamook Bays are modest (~ 1.0 m) but several cores sites in Tillamook Bay show about 1.5 m of subsidence from the last Cascadia Margin earthquake, now correlated to Japanese tsunami records at AD 1700 (Atwater et al., 2005) (Figure 8). The core records in Tillamook Bay do not demonstrate at least two events

of 1.5 m subsidence, thereby placing the trough of maximum subsidence landward of the eastern shoreline of Tillamook Bay.

Coseismic subsidence events in the Siuslaw estuary range from less than 0.5 m to 1.0–1.5 m over a landward distance of about 20 km (Figure 9). Sites of maximum subsidence (218 and 219) recorded near Mapleton, Oregon, occur at a distance of 120 km from the deformation front. The trough of maximum subsidence likely occurs within 10 km distance landward of sites 218 and 219. The trough of maximum subsidence in the Siuslaw locality is estimated to be located at distance of 130 km from the deformation front.

Multiple sites lacking evidence of episodic subsidence, as based on plant marcrofossils and microfossils [Briggs, 1994] occur in the lowermost reaches of the Siuslaw and Umpqua estuaries (Figures 9 and 10). These sites occur at distances of 100 ± 10 km from the deformation front. These core sites represent the zero-isobase between coseismic uplift and coseismic subsidence in the central part of the study area (Figure 16). The zero–isobase likely extends through the lowermost reaches of Coos Bay, but it is partially obscured by localized subsidence in South Slough and Pony Slough (Figure 11). The sources of the localized subsidence in Coos Bay are not known, but the South Slough occurs in a north–south syncline axis, possibly associated with underlying fault(s) [Madin et al., 1995].

Coseismic subsidence in the Coquille estuary ranges from 0.5-1.0 m at the coast to approximately 1.5m over a landward distance of about 20 km (Figure 12). The small values of coseismic subsidence in the lowermost reaches of the Coquille estuary reduce the number of expected subsidence events recorded in some wetland sites. The number of coseismic subsidence events increases with distance landward to Coquille, Oregon, where the river turns south. The trough of maximum subsidence likely occurs landward of site 521, at an estimated distance of about 100 km from the deformation front.

Comparison of Geologic Strain Records

A map of the estimated position of the trough of maximum subsidence in the Columbia River, Siuslaw, and Coquille estuary localities suggests a significant narrowing of the coupled zone with distance south in the study area (Figure 17). The distance between the trough of maximum subsidence and the deformation front decreases from 150 to 100 km between the Columbia and Coquille drainages.

Nevertheless, the position of the zero-isobase at 100 km from the deformation front in the south central part of the study area confirms the presence of a relatively wide zone of strong interplate–coupling throughout the length of the South Central Cascadia Margin.

The landward edge of the Quaternary deformation belt, based on offshore seismic profiling (Figure 3) and onshore terrace deformation (Table 2 and Figure 6) ranges from about 110 km to about 80 km distance from the deformation front between the Columbia River and Coos Bay, respectively (Figure 17). The landward edge of the Quaternary deformation belt approximately coincides with the late Holocene zero–isobase in the south central part of the study area, though some inferred upper plate structures appear to occur well landward of the zero-isobase in Coos Bay, as based on localized late Holocene subsidence (Figure 11). The landward edge of the late Neogene deformation belt also extends somewhat landward of the the zero–isobase in the south central part of the study area. The similarities in

positions of all three strain indicators demonstrates the presence of a relatively wide interplate coupled zone throughout the 500 km length of the South Central Cascadia Margin.

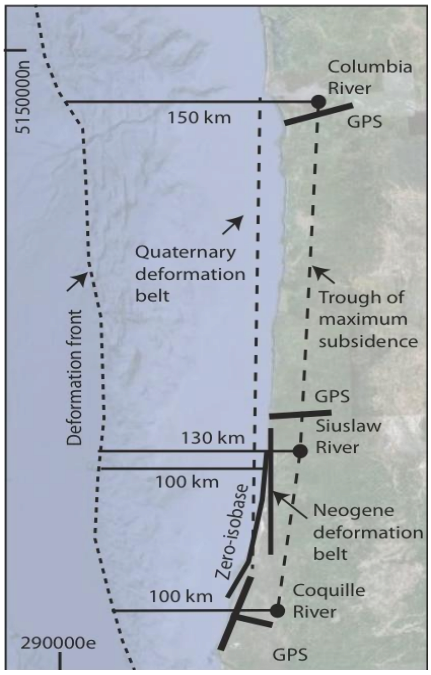

Figure 17. Map of the South Central Cascadia Margin showing deformation front (dotted line), estimated position of the trough of maximum subsidence (bold dashed line) with distances from the deformation front, and the zero-isobase (solid line) with distance from the deformation front in the south central part of the study area. GPS baselines localities are shown with baseline positions (bold lines) The landward edge of the Quaternary deformation belt (medium dashed line) is shown for most of the study area. The landward edge of the late Neogene deformation belt (solid bold line) is shown for the south central part of the study area.

Preliminary analyses of the GPS station baselines (Figure 17) establish modern west–east shortening rates of about 5 mm yr^{-1} normalized to 40 km baseline lengths in the north and central coast. The north and central coast baselines are located within the zone of elastic strain in the upper plate. Baseline shortening rates in the south coast are about twice as large as those in the north and central coast localities. The mid-point distances of the south coast baselines are about 60–70 km from the deformation front. The larger shortening rates in the south coast baselines might reflect their proximity to the interplate coupled zone, which approaches or underlies the south coast baselines. Additional work is underway to analyze many more coastal GPS strain records that have been collected in the South Central Cascadia Margin.

CONCLUSION

Four different time scale records of coastal deformation in the South Central Cascadia Margin demonstrate convergent tectonic strain associated with active subduction of the Juan

De Fuca plate under the North American plate. These strain records refute some previous studies, which suggested that only aseismic creep or decoupled plate subduction occurs in the South Central Cascadia Margin. Two of the coastal deformation records presented here demonstrate long–term inelastic strain during the late Neogene and late Pleistocene. The inelastic strain records extend 90-110 km landward of the buried trench or deformation front in the south central part of the study area, near Florence, Oregon. These records imply strong long term coupling of the interplate megrathrust to distances of 100 km landward of the deformation front. Episodic rupture of the wide coupled zone could lead to large magnitude subduction zone earthquakes and associated nearfield tsunami inundations in the South Central Cascadia Margin.

Coseismic subsidence ranges from at least 1.5 m to less than 0.5 m of abrupt sea level rise in the study area coastal marshes. The maximum trough of coseismic subsidence (> 1.5 m subsidence) occurs at distances of 150 to 100 km from the deformation front, decreasing from north to south in the study area. The zero–isobase (< 0.5 m coseismic subsidence) occurs at a distance of about 100 km from the deformation front, in the south central part of the study area. The position of the zero–isobase is very well constrained in several tidal marsh systems during the last several thousand years. The zero–isobase is assumed to reflect the width of the coupled zone, about 100 km landward distance from the deformation front in the south central part of the study area, near Florence, Oregon. The predicted strengths of seismic shaking, both on the coast and in the more densely populated forearc valleys that are located landward of the coast, depend, in part, on the assumed landward extent of the coupled zone. Building codes are established on the basis of the predicted strengths of seismic shaking, so they are also dependent on the assumed width of the coupled zone. The results presented here will have direct relevance to building code determinations in the South Central Cascadia Margin.

Late Holocene coastal wetlands establish elastic strain cycles, with six interseismic intervals between 3.2 and 0.3 ka averaging 480 years in duration. The two longest strain cycles average 850 years between recorded coseismic subsidence events. The two shortest strain cycles average only 200 years in length. The current interseismic strain cycle, starting at AD1700 is 300 years long. Policymakers are now confronted with indecision about the imminence of the next megrathrust rupture, which could be dependent on whether or not the current strain cycle is part of a cluster of short recurrence intervals. Interseismic uplift between earthquake events is measured in several coastal marsh systems, including Netarts Bay, Oregon. The net amount of measured interseismic uplift is not directly proportional to the length of the interseismic interval. It appears that most of the interseismic uplift occurs within the first couple of millennia following the preceding megathrust rupture. Based on the present high marsh development in most of the study area tidal basins it is expected that little or no additional marsh emergence will occur prior to the next megathrust rupture. The mechanism(s) leading to the observed decline of vertical strain accumulation in the zone of interseismic uplift during the later stages of the longer interseismic intervals are not known.

Modern horizontal strain or shortening is measured perpendicular to the coastline in three GPS baselines in the South Central Cascadia Margin. The measured strain, on the order of at least 0.5 cm per year over ~ 40 km long baselines, demonstrates active strain accumulation in the upper crust. Though small in magnitude the measured strain rates are consistent with a current condition of interplate coupling along the full length of the South Central Cascadia Margin. These are the first direct measurements of GPS baseline shortening made in the Central Cascadia Margin. These initial GPS results suggest declining strain with increasing

distance from the coupled zone, and a component of north– south shortening, possibly associated with oblique subduction or regional upperplate compression. Additional monitoring and statistical analyses of many more GPS baselines in the Central Cascadia Margin are underway to resolve the spatial variability of active tectonic strain in the Central Cascadia subduction zone.

ACKNOWLEDGMENTS

We thank Gregg Brigs, Chip Barnett, Charlie Clough, Betsy McLeod, Aaron Wieting, Chris Beard, and Gene Pierson for assisting with field work, laboratory analyses, and study logistics. Brian Atwater provided a useful review of an earlier version of this chapter. This Oregon Sea Grant project was funded by the NOAA Office of Sea Grant and Extramural Programs, US Department of Commerce, under grants number NA36RG0551 and NA36RG0451, project number R/CP-28, and by appropriations made by the Oregon State Legislature. Additional funding was provided through USGS NEHRP 14-08-0001-G1512 and NSF EAR8903903.

REFERENCES

Atwater, B. F. (1987). Evidence for great Holocene earthquakes along the outer coast of Washington State (US). *Science*, 236(4804), 942-944.

Atwater, B. F., and Hemphill-Haley, E. (1996). Preliminary estimates of recurrence intervals for great earthquakes of the past 3500 years at northeastern Willapa Bay, Washington. (*US Geological Survey Open-File Report 96-001*).

Atwater, B. F. (1994). Geology of the Holocene liquefaction features along the lower Columbia River at Marsh, Brush, Price, Hunting, and Wallace Islands, region and Washington (*US Geological Survey Open-File Report* 94-209).

Atwater, B. F., Musumi-Rokkaku, S., Satake, K., Tsuji, Y., Ueda, K., and Yamaguchi, D. K. (2005). The Orphan Tsunami of 1700. Reston, Virginia: US Geological Survey and University of Washington Press.

Atwater, B. F., Nelson, A. R., Clague, J. J., Carver, G. A., Yamaguchi, D. K., Bobrowsky, P. T., et al. (1995). Summary of coastal geologic evidence of past great earthquakes at the Cascadia subduction zone. *Earthquake Spectra*, 11(1), 1-18.

Baldwin, E. M. (1956), Geology map of the lower Siuslaw River area, Oregon, *US Geological Survey*, O. M.-186.

Baldwin, E. M. (1961), Geologic map of the lower Umpqua River area, Oregon, *US Geological Survey*, O. M.-204.

Baldwin, E. M. (1974), Eocene stratigraphy of southwestern Oregon. Oregon Department of Geology and Mineral Industries Bulletin 83, 40 p. 1 map.

Baldwin, E. M., J. D. Beaulieu, L. Ramp, J. Gray, V. C. Jr. Newton, and R. S. Mason, (1973), *Geology and mineral resources of Coos County, Oregon, Bulletin* 80. 82 pp., Oregon Department of Geology and Mineral Industries, Portland, Oregon.

Barnett, E. T. (1997). Potential for coastal flooding due to coseismic subsidence in the central Cascadia margin. Portland State University, Portland, Oregon.

Beaulieu, J. D., and Hughes, P. W. (1975). *Environmental geology of western Coos and Douglas Counties, Oregon* (Bulletin 87 No. 87). Portland, Oregon: Department of Geology and Mineral Industries.

Black, G. L. (Cartographer). (1993). Offshore-onshore geologic cross-section from the Pan American Corporation well (continental shelf) to the Umpqua River (southern Oregon Coast Range) [Open-File Report].

Blakely, R. J., Brocher, T. M., and Wells, R. E. (2005). Subduction-zone magnetic anomalies and implications for hydrated forearc mantle. *Geology*, 33, 445-448.

Bradley, C. C., and Griggs, G. (1976). Form, genesis, and deformation of central California wave-cut platforms. *Geological Society of America Bulletin*, 87, 433-449.

Briggs, G. G. (1994). Coastal crossing of the elastic strain zero-isobase, Cascadia margin, south-central Oregon coast. Portland State University, Portland, Oregon.

Clarke, S. H., and Carver, G. A. (1992). Late Holocene tectonics and paleoseismicity, southern Cascadia subduction zone. *Science*, 255, 188-192.

Clifton, H. E. (1994). Transgressive and early highstand systems tracts: Pleistocene terrace deposits Willapa Bay, Washington. Paper presented at the Field Trip Guide S. E. P. M. Research Conference: Clastic Deposits of the Transgressive Systems Tract, Long Beach, Washington.

CORS. (2011). N. O. A. A. Continuously Operating Reference Stations Data Center. *http://www.ngs.noaa.gov/CORS/.*

Darienzo, M. E., 1987, M. S., Late Holocene geologic history of a Netarts salt marsh, northwest Oregon coast, and its relationship to relative sea level changes. M. S. *Thesis, University of Oregon, Eugene, Oregon*, 94 p.

Darienzo, M. E., 1991, Ph. D., Late Holocene paleoseismicity along the northern Oregon coast. Ph. D. *Thesis, Portland State University, Portland, Oregon*, 167 p.

Darienzo, M. E., and Peterson, C. D. (1987). Netarts Marsh: Subduction zone earthquakes or super-storms. Symposium: Could there be a devastating earthquake in Oregon. Paper presented at the Oregon Academy of Science, Monmouth, Oregon.

Darienzo, M. E., and Peterson, C. D. (1990). Episodic tectonic subsidence of Late Holocene salt marshes, northern Oregon central Cascadia margin. *Tectonics*, 9(1), 1-22.

Darienzo, M. E., Peterson, C. D., and Clough, C. (1994). Stratigraphic evidence for great subduction zone earthquakes at four estuaries in Northern Oregon. *Journal of Coastal Research*, 10(4), 850-876.

Goldfinger, C., Kulm, L. D., Yeates, R. S., Appelgate, B., MacKay, M. E., and Moore, G. F. (1992a). Transverse structural trends along the Oregon convergent margin: Implications for Cascadia earthquake potential and crustal rotations. *Geology*, 20(2), 141-144.

Goldfinger, C., Kulm, L. D., Yeats, R. S., Appelgate, B., MacKay, M. E., and Cochrane, G. R. (1996). Active strike slip faulting and folding of the Cascadia plate boundary and forearc in central and northern Oregon. In A. M. Rogers, W. J. Kochelman, G. R. Priest and T. J. Walsh (Eds.), Assessing and reducing earthquake hazards in the Pacific Northwest
(Vol. *US Geological Survey Professional Paper* 1560, pp. 223-256).

Goldfinger, C., Kulm, L. D., Yeats, R. S., Mitchell, C. E., Weldon, R. J., III, Peterson, C. D., et al. (1992b). Neotectonic map of the Oregon continental margin and adjacent abyssal

plain (Open File Report 0-92-4). Portland, Oregon: Oregon Department of Geology and Mineral Industries.

Goldfinger, C., Grijalva, K., Bürgmann, R., Morey, A. E., Johnson, J. E., Hans Nelson, C., Gutiérrez-Pastor, J., Ericsson, A., Karabanov, E., Chaytor, J. D., Patton, J., and Gràcia, E. (2008). Late Holocene Rupture of the Northern San Andreas Fault and Possible Stress Linkage to the Cascadia Subduction Zone. *Bulletin of the Seismological Society of America*, 98, 861–889, doi: 10.1785/0120060411.

Hyndman, R. D., and Wang, K. (1995). The rupture zone of the Cascadia great earthquakes from current deformation and thermal regime. *Journal of Geophysical Research*, 100, 22133-22154.

Kelsey, H. M. (1990). Late Quaternary deformation of marine terraces on the Cascadia subduction zone near Cape Blanco, Oregon. *Tectonics*, 9, 983-1014.

Kelsey, H. M., Nelson, A. R., Hemphill-Haley, E., and Witter, R. C. (2005). Tsunami history of an Oregon coastal lake reveals a 4600 yr record of great earthquakes in the Cascadia subduction zone. *Geological Society of America Bulletin*, 117(7/8), 1009-1032.

Kelsey, H. M., Witter, R. C., and Hemphill-Haley, E. (2002). Plate-boundary earthquakes and tsunamis of the past 5500 yr, Sixes River estuary, southern Oregon. *Geological Society of America Bulletin*, 114(3), 298-134.

Kennedy, G. L., Kajoie, K. R., and Wehmiller, J. F. (1982). Aminostratigraphy and faunal correlations of late Quaternary marine terraces, Pacific coast, US. *Nature*, 299, 545-547.

Li, W. (1992). Evidence for late Holocene coseismic subsidence in the lower Eel River valley, Humboldt county, northern California: An application of foraminiferal zonation to indicate tectonic submergence. Humboldt State University, Arcata, California.

Madin, I. P., McInelly, G. W., and Kelsey, H. M. (Cartographer). (1995). Geologic map of Charleston Quadrangle, Coos County, Oregon.

McInelly, G. W., and Kelsey, H. M. (1990). Late Quaternary tectonic deformation in the Cape Arago-Bandon region of coastal Oregon as deduced from wave-cut platforms. *Journal of Geophysical Research*, 95, 6699-6713.

McNeil, L. C., Goldfinger, C., Yeates, R. S., and Kulm, L. D. (1998). The effects of upper plate deformation on records of prehistoric Cascadia subduction zone earthquakes. In I. S. Stewart and C. Vita-Finzi (Eds.), *Coastal Tectonics* (Vol. 146, pp. 321-342). London: Geological Society of London.

Muhs, D. R., Kelsey, H. M., Miller, G. H., Kennedy, G. L., Whelan, J. F., and McInelly, G. W. (1990). Age estimates and uplift rates for late Pleistocene marine terraces: Southern Oregon portion of the Cascadia forearc. *Journal of Geophysical Research*, 95, 6685-6698.

Mulder, R. A. (1992). Regional tectonic deformation of the northern Oregon coast as recorded by Pleistocene marine terraces. Portland State University, Portland, Oregon.

Nelson, A. R. (1987). Apparent gradual rise in relative sea level on the south-central Oregon coast during late Holocene-implications for the great Casdadia earthquake hypothesis. E. O. S., 68, 1240.

Nelson, A. R. (1992). Discordant 14C ages from buried tidal-marsh soils in the Cascadia subduction zone, southern Oregon coast. *Quaternary Research,* 38, 74-90.

Nelson, A. R., Jennings, C. W., and Kashima, A. E. (1996). An earthquake history derived from stratigraphic and microfossil evidence of relative sea-level change at Coos Bay, southern coastal Oregon. *Geological Society of America Bulletin*, 108, 141-154.

Newton, V. C., Jr. (Cartographer). (1980). Prospects for oil and gas in the Coos Basin, Western Coos, Douglas, and Lane Counties, Oregon.

Niem, A. R., and Niem, W. A. (Cartographer). (1985). Oil and Gas investigations of the Astoria Basin, Clatsop and northernmost Tillamook Counties, northwest Oregon [OGI-14].

Personius, S. F. (1993). Age and origin of fluvial terraces in the central Coast Range, Western Oregon (Bulletin 2038): US Geological Survey.

Personius, S. F. (1995). Late Quaternary stream incision and uplift in the forearc of the Cascadia subduction zone, western Oregon. *Journal of Geophysical Research*, 100, 20193-20210.

Peterson, C. D., Barnett, E. T., Briggs, G. G., Carver, G. A., Clague, G., and Darienzo, M. E. (1997). Estimates of coastal subsidence from great earthquakes in the Cascadia subduction zone, Vancouver Island B. C., Washington, Oregon, and Northernmost California (Open-File Report 0-07-5): Oregon Geology and Mineral Industries.

Peterson, C. D., Carver, G., Cruikshank, K. M., Abramson, H., Garrison-Laney, C., Dengler, L., 2011. Evaluation of the use of paleotsunami deposits to reconstruct inundation distance and runup heights associated with prehistoric inundation events, Crescent City, southern Cascadia margin. *Earth Surface Processes and Landforms*. DOI:10.1002/esp.2126.

Peterson, C. D., Cruikshank, K. M., Schlichting, R. B., and Braunsten, S., 2010, Distal Runup Records Of Latest Holocene Paleotsunami Inundation In Alluvial Flood Plains: Neskowin and Beaver Creek, Oregon, Central Cascadia Margin, US, *Journal of Coastal Research*, 26:622-634. Doi 10.2112/08-1147.1

Peterson, C. D., Cruikshank, K. M., Jol, H. M., Schilichting, R. B., 2008, Minimum runup heights of paleotsunami from evidence of sand ridge overtopping at Cannon Beach, Oregon, Central Cascadia Margin, US, *Journal of Sedimentary Research*, v. 78, p. 390-409.

Peterson, C. D., and Darienzo, M. E. (1997). Discrimination of flood, storm and tectonic subsidence events in coastal marsh records of Alsea Bay, Central Cascadia Margin, US. In A. M. Rogers, T. J. Walsh, W. J. Kockelman and G. R. Priest (Eds.), Assessing and Reducing Earthquake Hazards in the Pacific Northwest (Vol. *U. S. G. S. Professional Paper* 1560, pp. 115-146).

Peterson, C. D., Darienzo, M. E., Doyle, D. L., and Barnett, E. T. (1995). Evidence for coseismic subsidence and tsunamis inundation during the past 3000 years at Siletz Bay, Oregon. In G. R. Priest (Ed.), *Explanation of mapping methods and use of the tsunami hazard map of the Siletz Bay area, Lincoln County, Oregon* (Vol. O-95-05, pp. 45-69). Portland, Oregon: Oregon Department of Geology and Mineral Industries.

Peterson, C. D., Darienzo, M. E., Hamilton, D., Pettit, D. J., Yeager, R. K., Jackson, P. L., et al. (1994). Cascadia Beach-Shoreline Data Base, Pacific Northwest Region, US (Open-File Report 0-94-2): Oregon Department of Geology and Mineral Industries.

Peterson, C. D., Doyle, D. L., and Barnett, E. T. (2000). Coastal flooding and beach retreat form coseismic subsidence in the central Cascadia Margin, US. *Environmental and Engineering Geoscience*, 6(3), 255-269.

Peterson, C. D., Komar, P. D., and Scheidegger, K. F. (1986). Distribution, geometry, and origin of heavy minearl placer deposits on Oregon beaches. *Journal of Sedimentary Petrology*, 56(1), 67-77.

Peterson, C. D., and Priest, G. R. (1995). Preliminary reconnaissance survey of Cascadia paleotsunami deposits in Yaquina Bay, Oregon. *Oregon Geology,* 57, 33-40.

Peterson, C. D., Stock, E., Cloyd, C., Beckstrand, D., Clough, C., Erlandson, J., et al. (2006). Dating and morphostratigraphy of coastal dune sheets from the central west coast of North America. Corvallis, Oregon: Oregon Sea Grant Publications.

Peterson, C. D. and K. F. Scheidegger, 1984. Holocene depositional evolution in a small active- margin estuary of the northwestern United States. *Mar. Geol.*, 59:51-83.

Peterson, C. P., and Gray, J. J. (Cartographer). (1986). Geologic map of the ocean floor off Oregon and adjacent continental margin [GMS-42].

PANGA. (2011). Pacific Northwest Geodetic Array Data Center. *http://www.geodesy.cwu.edu/.*

Priest, G. R., Myers, E., Baptista, A. M., Fleuck, P., Wang, K., Kamphaus, R. A., et al. (1997). Cascadia subduction zone tsunamis: Hazard mapping at Yaquina Bay, Oregon (Open-File Report No. O-97-34). Portland, Oregon: Oregon Department of Geology and Mineral Insustries.

Priest, G. R., Myers, E., Baptista, A. M., Fleuck, P., Wang, K., and Peterson, C. D. (2000). Source simulation for tsunamis: Lessons learned from fault rupture modeling of the Cascadia subduction zone, North America. Science of Tsunami Hazards.

R. Development Core Team (2011). R: A language and environment for statistical computing. R Foundation for Statistical Computing, Vienna, Austria. ISBN 3-900051-07-0, *URL http://www.R-project.org/*.

Saltus, R. W., Blakely, R. J., Hauessler, P. J., and Wells, R. E. (2005). Utility of aeromagnetic studies for mapping potentially active faults in two forearc basins: Puget Sound, Washington, and Cook Inlet, Alaska. *Earth, Planets, Space*, 57, 781-793.

Satake, K., Wang, K., and F., A. B. (2003). Fault slip and seismic moment of the 1700 Cascadia earthquake inferred from Japanese tsunami descriptions. *Journal of Geophysical Research*, 108(11), ESE 7-1 - ESE 7-17.

Schlicker, H. G., and Deacon, R. J. (1974). Environmental Geology of Coastal Lane County, Oregon (Bulletin 85 No. 85). Portland, Oregon: Department of Geology and Mineral Industries.

Shennan, I., Long, A. J., Rutherford, M. M., Innes, F. M., Green, F. M., and Walker, K. J. (1998). Tidal marsh stratigraphy, sea-level change and large earthquakes: Submergence events during the last 3500 years at Netarts Bay, Oregon, US. *Quaternary Science Reviews*, 17, 365-393.

Snavely, P. D. Jr., N. S., MacLeod, and H. C., Wagner (1972a), Preliminary bedrock geologic map of the Yaquina and Toledo quadrangles, Oregon. *US Geological Survey open-file map*.

Snavely, P. D. Jr., N. S., MacLeod, and H. C., Wagner (1972b), Preliminary bedrock geologic map of the Cape Foulweather and Euchre Mountain quadrangles, Oregon. *US Geological Survey open-file map*.

Stuiver, M., Reimer, P. J., and Reimer, R. W. (2005). C. A. L. I. B. 5.0: *http://calib.qub.ac.uk/calib/*.

Ticknor, R. L. (1993). Late Quaternary crustal deformation on the central Oregon coast as deduced from uplifted wave-cut platforms. Western Washington University, Bellingham, Washington.

Tolman, B., Harris, R. B., Gaussiran, T., Munton, D., Little, J., Mach, R., et al. (2004). *The GPS Toolkit -- Open Source GPS Software*. Paper presented at the Proceedings of the 17th International Technical Meeting of the Satellite Division of the Institute of Navigation (ION GNSS 2004).

Valentine, D. W. (1992). Late Holocene stratigraphy, Humboldt Bay, California, Evidence for late Holocene paleoseismicity of the southern Cascadia subduction zone. Humboldt Sate University, Arcadia, California.

Venables, W. N. and Ripley, B. D. (2002) *Modern Applied Statistics with S. Fourth Edition*. Springer, New York. ISBN 0-387-95457-0.

Wells, R. E. (1990). Paleomagnetic roations and the Cenozoic tectonics of the Cascade arc, Washington, Oregon, and California. Journal *of Geophysical Research*, 95(B12), 19409-19417.

West, D. O., and McCrumb, D. R. (1988). Coastline uplift in Oregon and Washington and the nature of Cascadia subduction zone tectonics. *Geology*, 16(2), 169-172.

Witter, R. C., Kelsey, H. M., and Hemphill-Haley, E. (2003). Great Cascadia earthquakes and tsunamis of the past 6700 years, Coquille River estuary, southern coastal Oregon. *Geological Society of America Bulletin*, 115, 1289-1306.